https://doi.org/10.26599/FRICT.2026.9441243

Review Article

Tribological mechanisms and performance optimization strategies of cemented carbides under extreme service conditions

Kaipeng Zhang, Pengpeng Bai*, Hui Cao, Yonggang Meng**

State Key Laboratory of Tribology in Advanced Equipment, Tsinghua University, Beijing 100084, China

* Corresponding author.

** Corresponding author.

E-mail address: baipengpeng@mail.tsinghua.edu.cn (P. Bai), mengyg@tsinghua.edu.cn (Y. Meng)

Received: November 12, 2025; Revised: January 28, 2026; Accepted: March 9, 2026

Abstract: Cemented carbides, composed of hard carbide phases and metallic binders, are extensively employed in extreme tribological environments involving high-load dry friction, elevated-temperature cutting, erosive particle flows, cyclic impact, micro-vibration, and corrosive media. In response to increasing performance demands under such complex service conditions, this review systematically evaluates the tribological behaviors and failure mechanisms of cemented carbides under adhesive, abrasive, fatigue-induced, oxidative, erosive, fretting, and corrosion-induced wear conditions. The critical influence of carbide phase type and grain scale, binder chemistry and mean

free path, and microstructural configuration on interfacial degradation pathways is clarified, establishing a structure-driven, mechanism-based framework that links microstructural descriptors with damage evolution and dominant wear modes. On this basis, multi-scale strengthening strategies-including compositional design, microstructural refinement, binder phase optimization, grain-scale engineering, PVD/CVD thin films, and surface texturing-are summarized and comparatively assessed with respect to their effectiveness across varied tribological conditions. Finally, emerging trends are discussed, with emphasis on multi-field coupling mechanisms, cross-scale wear modeling, low-Co and environmentally benign binder systems, powder-metallurgy-enabled, and adaptive surface engineering. This review provides theoretical guidance and design strategies for achieving high reliability and long-term service durability of sintered cemented carbides in extreme tribological environments.

Keywords: Cemented carbide, Friction and wear, Tribological properties, Surface engineering, Performance optimization.

1. Introduction

Cemented carbide is a class of high-performance composite materials prepared by powder metallurgy, in which high-melting-point metal carbides serve as the hard phase, while metals such as Co or Ni act as the binder phase. Owing to their high hardness, excellent wear resistance, and high elastic modulus, these materials can maintain favorable thermal stability and oxidation resistance under elevated temperatures, while also exhibiting resistance to thermal shock and softening **[1]**. These comprehensive properties endow cemented carbides with high service reliability under extreme loads and harsh environments. At the microstructural level, the hard phase imparts exceptionally high hardness and wear resistance, whereas the binder phase provides the necessary toughness and interfacial bonding strength. The synergistic effect between carbides and the metallic binder phase ensures that cemented carbides can achieve a

balance of strength and toughness under complex stress conditions. In addition, microstructural parameters such as grain size, binder phase distribution, and interfacial stability play a decisive role in governing the wear behavior and environmental adaptability of the material **[2]**.

Cemented carbides, owing to their outstanding comprehensive mechanical properties, have been widely employed under various extreme service conditions. In the field of mechanical manufacturing, their wear resistance and resistance to thermal softening are primarily utilized for high-speed cutting tools and the machining of complex curved surfaces (as shown in **Fig.1**) **[3]**. In mining and geological exploration, drill bits, roller cones, and cutting teeth made of cemented carbides exhibit impact resistance and long service life, enabling them to withstand high-stress rock-breaking environments. In the aerospace industry, cemented carbides are employed in nozzles, turbine blades, and combustion components, where their high-temperature resistance and thermal shock resistance ensure the stable operation of engines under extreme thermal conditions **[4]**. In marine engineering, this material is employed in deep-sea drilling tools and pipeline cutting devices due to its favorable corrosion and erosion resistance, thereby significantly enhancing service life and operational reliability. As a key fundamental material in advanced manufacturing systems, cemented carbides hold an irreplaceable strategic position in equipment manufacturing, energy development, and the defense industry **[5]**. The service performance of cemented carbides is directly related to the lifespan and safety of major engineering equipment. Consequently, research on their service reliability, failure mechanisms, and surface modification technologies has become a critical direction for overcoming bottlenecks in key materials, ensuring national industrial security, and supporting the strategic development of the energy sector **[6]**.

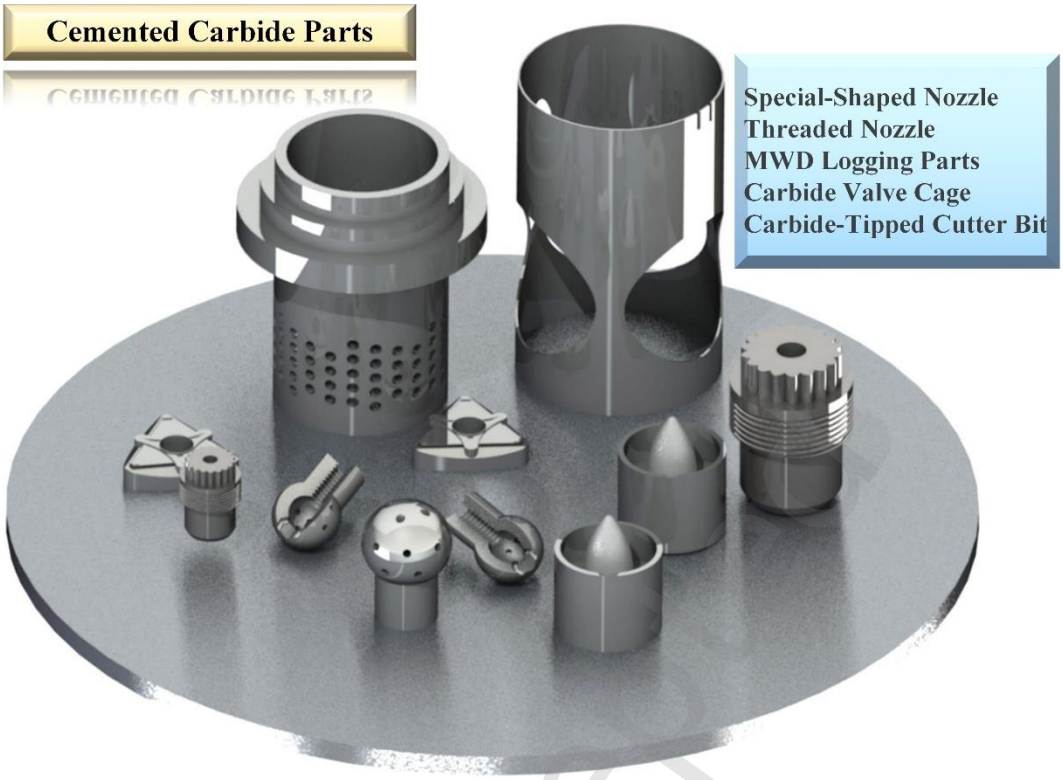

Fig.1 Examples of typical complex cemented carbide parts: special-shaped nozzle, threaded nozzle, measurement while drilling (MWD) logging parts, carbide valve cage and carbide-tipped cutter bit. All samples were produced through PM methods, plus postprocessing (grinding and polishing) (adapted from Ref. **[3]**)

Under such multi-field coupled conditions, the performance degradation of cemented carbides essentially occurs at the frictional contact interface and is dominated by the synergistic effect of mechanical load, thermal effect and chemical-electrochemical reactions under sliding conditions. These interactions lead to a tribo-induced dynamic evolution of the contact interface, which plays a central role in controlling the degradation behaviors **[7]**. In addition to conventional adhesive, abrasive, and fatigue wear, oxidative and corrosion-induced damage further accelerates material deterioration. Among these failure modes, corrosion-wear has emerged as a critical coupled degradation mechanism in marine, chemical, and high-humidity environments **[8]**. During the wear process, the friction-induced electrochemical reactions promote the localized dissolution of the binder phase, thereby weakening the load-bearing capacity of the carbide-binder interface. In addition, the carbide fragments generated by the interface spalling as the third body abrasive particles, repeatedly participating in

the shear and load transfer within the contact zone, further amplifying the mechanical wear effect. In-situ electrochemical friction tests indicate that the chemical composition, grain size and interface structure of the binder phase determine the tribological behavior under corrosion-wear by regulating the interfacial reactivity, the formation and evolution of the third-body layer **[9]**.

Despite considerable progress in elucidating wear mechanisms and improving material formulations, several critical scientific and engineering challenges remain unresolved under extreme tribological conditions **[10]**. Under combined sliding contact and electrochemical conditions, the mechanisms by which electrochemical dissolution of the binder phase evolves into carbide detachment and interfacial failure under frictional shear and cyclic loading remain insufficiently understood. In particular, the micro-damage evolution pathways at the carbide/binder interface under the coupled effects of potential fluctuations and cyclic loading have not yet been clearly elucidated **[11]**. Meanwhile, the existing wear and degradation models are still difficult to quantitatively capture the complex coupling among contact stress, temperature variation, corrosive media and tribological behavior under sliding conditions, which limits the reliable prediction of long-term service life **[12]**. In addition, the carbide morphology, interfacial bonding chemistry and residual stress evolution synergistically regulate the wear-corrosion kinetics by affecting third-body layer stability, interfacial shear behavior and crack propagation paths. However, the underlying mechanisms have not yet formed a unified understanding **[13, 14]**. On the materials side, the traditional Co/Ni binder phases exhibit limited chemical stability in marine, acidic and humid environments. Although alternative approaches, such as corrosion-resistant alloy binder phase, gradient structures and high-entropy or nanocomposite interfacial systems, have been proposed, their tribological performances remain insufficiently validated **[15]**. Moreover, most existing investigations are limited to short-duration laboratory tests and are devoid of in-situ characterization techniques capable of capturing real-time interfacial evolution, leaving time-dependent degradation mechanisms largely unexplored **[16]**. Finally, the lack of unified tribological evaluation metrics, standardized accelerated degradation testing protocols and cross-scale databases

continues to hinder the development of robust correlations among organization, performance, and service life **[17]**. In summary, overcoming these challenges requires multidisciplinary efforts that integrate interfacial degradation mechanisms, multi-physics modeling, advanced binder system design, and real-time monitoring techniques to enable the reliable application of cemented carbides in extreme environments **[18, 19]**.As illustrated in **Fig.2**, WC-based binder systems have evolved from traditional Co-based binders-characterized by superior wettability and metallurgical compatibility, yet limited by high cost, biotoxicity, and poor corrosion stability. Ni-based binders, which offer enhanced corrosion resistance but weaker WC interfacial bonding.

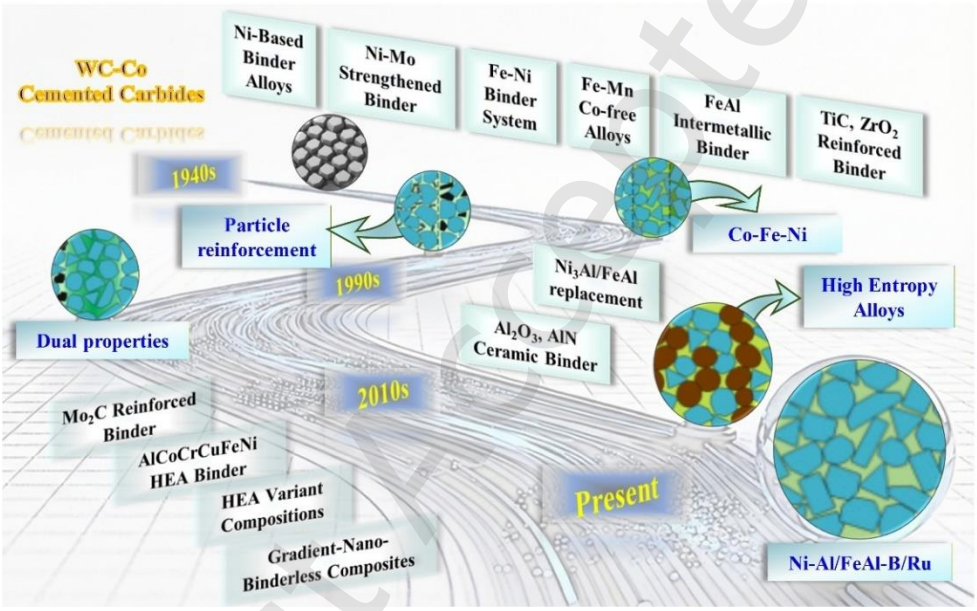

Fig.2 Evolutionary pathway of binder systems in WC-based cemented carbides (adapted from Ref. **[20]**).

Over recent decades, cemented-carbide research has moved beyond WC-Co toward low-/Co-free systems, multicomponent binders, and graded microstructures. However, key mechanistic links remain unclear. Unified criteria for the shift from oxidation-dominated wear to abrasion-assisted delamination at high temperature are still lacking. In wear-corrosive environments, binder-selective dissolution and WC-binder interfacial degradation can accelerate wear nonlinearly, yet transferable structure-pathway correlations remain limited. Moreover, in multi-field contacts, third-body evolution is tightly coupled with subsurface cyclic damage, which is not well captured by wear-mode-isolated descriptions.

This review provides a comprehensive and systematic analysis of the tribological behavior of sintered cemented carbides under extreme service conditions, encompassing both corrosion-induced and non-corrosive wear mechanisms. Specifically, it examines high-stress abrasive wear, impact/fatigue wear, high-temperature oxidative wear, particle erosion, and corrosion-wear coupling, with particular attention to how multi-field environments involving stress, temperature, chemical/electrochemical reactions, and dynamic loading govern degradation pathways. The schematic framework of tribological research methodology for cemented carbides as shown in **Fig.3(a)**. Furthermore, the review highlights the microstructural influences of carbide morphology, binder chemistry, phase distribution, and interfacial stability on failure evolution. It also summarizes current optimization strategies, including binder alloy design, graded and nanocomposite architectures, surface engineering, and environment-specific reinforcement techniques. In addition, emerging research trends are discussed, such as in-situ degradation monitoring, data-driven and multi-scale tribological modeling, and the development of chemically inert, electrically stable, and high-bonding binder systems. These insights are expected to contribute to the design of next-generation cemented carbides with superior reliability and extended service lifetimes in harsh marine, aerospace, mining, and energy environments.

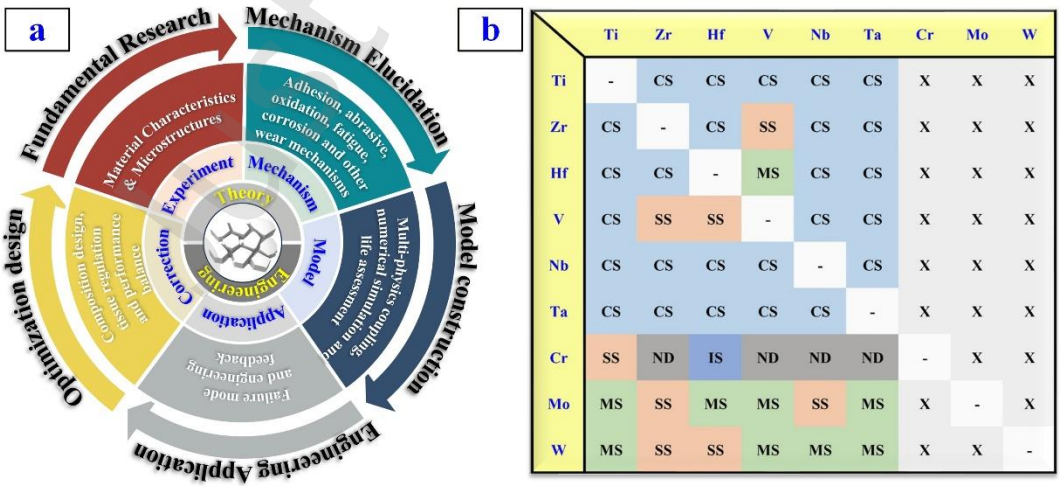

	Ti	Zr	Hf	V	Nb	Ta	Cr	Mo	W
Ti	-	CS	CS	CS	CS	CS	X	X	X
Zr	CS	-	CS	SS	CS	CS	X	X	X
Hf	CS	CS	-	MS	CS	CS	X	X	X
V	CS	SS	SS	-	CS	CS	X	X	X
Nb	CS	CS	CS	CS	-	CS	X	X	X
Ta	CS	CS	CS	CS	CS	-	X	X	X
Cr	SS	ND	IS	ND	ND	ND	-	X	X
Mo	MS	SS	MS	MS	SS	MS	X	-	X
W	MS	SS	SS	MS	MS	MS	X	X	-

Fig.3 (a) Schematic framework of tribological research methodology for cemented carbides, (b) Mutual Solubility of Refractory Carbides from Group IV, V, and VI. Abbreviations: CS represents completely soluble, MS represents mostly soluble, SS represents slightly soluble, ND represents no data, and X = does not form a cubic

structure **[11]**.

2. Overview of Cemented Carbide Materials

2.1 Definition and Classification of Cemented Carbides

Cemented carbides are ceramic-metal composites formed by consolidating high-hardness transition metal carbides and ductile metallic binders through powder metallurgy densification (as shown in **Fig.3(b)**) **[11, 20]**. In this system, the hard phase provides load-bearing capacity and wear resistance, while the binder phase enhances toughness and interfacial cohesion. To achieve performance matching and failure risk control under specific service conditions, the present work classifies cemented carbides according to these three dimensions (see **Table.1**).

Hard-phase classification determines chemical stability, thermo-mechanical resistance, and dominant wear mechanisms. WC is the most widely used carbide due to its high hardness and thermal stability. TiC and Ti(C, N) are typically introduced to increase oxidation and diffusion wear resistance at elevated temperatures, whereas TaC and NbC enhance thermo-chemical stability under aggressive environments.

Table.1 Classification and characteristics of cemented carbides based on material composition and grain size

Classification Dimension	Subcategory	Key Characteristics	Typical Application Areas
Hard Phase Type	WC	High hardness, excellent thermal stability, strong toughness	General machining, mining tools, aerospace components
	TiC	High chemical stability, heat resistance, corrosion resistance, brittle	High-temperature components, corrosive machining, composite coatings
	TiCN	High hardness, combines properties of TiC and TiN, superior wear resistance	High-end cutting tools, PVD coatings
	TaC/NbC	High melting point, strong oxidation resistance, chemically inert	Metallurgical dies, nuclear components, aerospace heat-resistant parts

Binder Phase Type	Co	Excellent wettability, strong metallurgical bonding, widely used	General hardmetals
	Ni	Excellent corrosion and oxidation resistance	Aerospace, marine engineering
	Fe:	Low cost, easy processing, applied in non-critical applications	Geological drilling, civilian tools
	HEA	Multi-element reinforcement, high structural stability, balanced properties	Extreme service conditions, advanced components
Grain Size	More than1μm	Cost-effective, moderate strength, stable processing	Standard cutting tools
	0.1-1 μm	Balanced strength and toughness, appropriate for general-purpose cutting operations	High-speed milling tools, impact-resistant tools
	Less than 0.1 μm	Extremely hard, excellent wear resistance, relatively brittle	Ultra-precision machining, microstructures, high-frequency wear zones

Grain size reflects the trade-off between hardness and toughness. Coarse-grained carbides (>1 μm) provide higher fracture toughness and are suitable for heavy-load wear applications. Fine-grained structures (0.5-1 μm) enable a balance between strength and toughness and are most commonly used in cutting tools. In summary, the classification of cemented carbides based on hard-phase composition, binder-phase chemistry, and grain-scale hierarchy provides a microstructural framework for performance tailoring. This classification system enables application-oriented optimization under high-temperature, high-stress, and corrosive service environments.

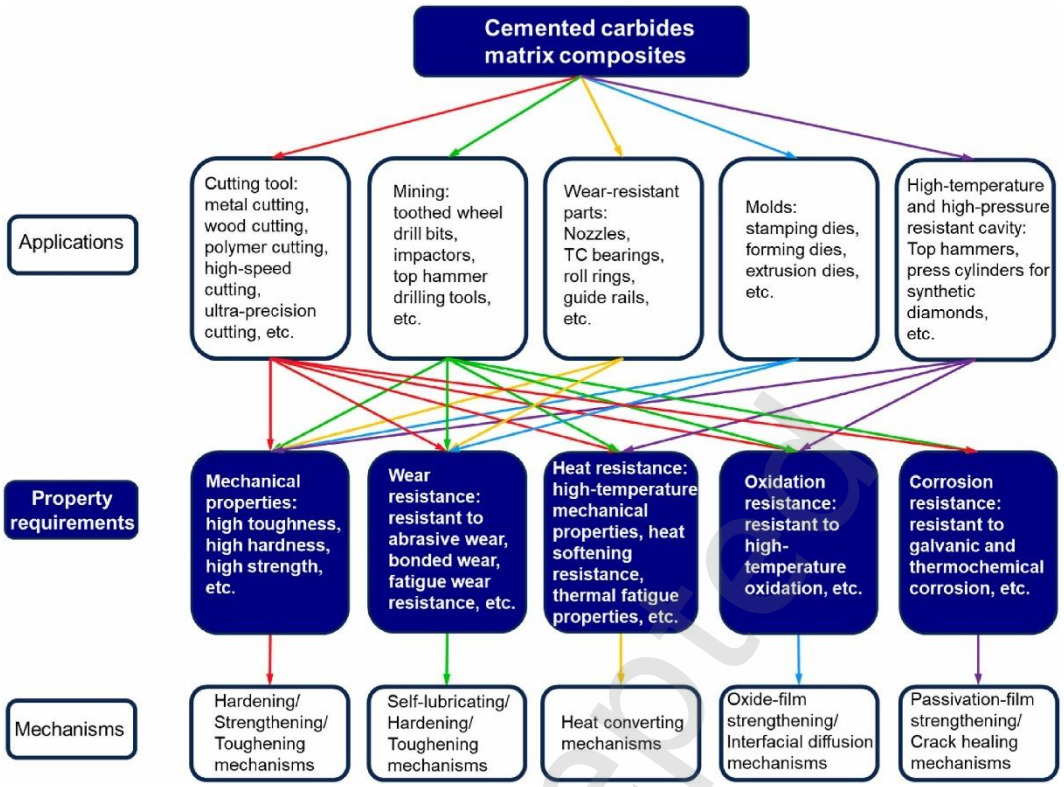

Fig.4 Schematic indicating applications, pivotal properties, and principal mechanisms of cemented carbides materials (adapted from Ref. **[64]**).

As shown in **Fig.4**, different application scenarios of cemented carbides are associated with distinct property requirements and degradation mechanisms. This application-driven perspective complements the compositional and microstructural classification discussed above and provides a contextual basis for the subsequent sections addressing microstructure, tribological behavior, corrosion-wear performance, and surface protection strategies.

2.2 Microstructure of Cemented Carbides

The microstructural architecture and compositional configuration of cemented carbides fundamentally determine their strength, wear resistance, and environmental stability. Typically, they consist of a hard ceramic phase embedded in a metallic binder (e.g., Co), where the ceramic skeleton provides load-bearing capacity and the binder contributes ductility.

Compositional optimization plays a crucial role in performance enhancement. WC is widely used for its hardness and thermal stability, but exhibits limited oxidation resistance at elevated temperatures. Secondary carbides such as TiC, TaC, and NbC

promote solid-solution strengthening, grain refinement, and suppression of abnormal WC growth, thus enhancing high-temperature wear resistance. Gradient structural design has also proven effective. For instance, Long et al. **[21]** prepared Ti(C, N)-based gradient cermets via powder-extrusion additive manufacturing, forming a core–shell architecture with uniform phase distribution and improved interfacial bonding. The sintered material achieved a relative density of 97.13%, with a hardness of 1760 HV, fracture toughness of 8.5 $MPa \cdot m^{1/2}$, and flexural strength of 2047 MPa, confirming the synergistic enhancement of hardness, strength, and toughness through gradient design. The binder phase critically affects toughness and degradation behavior **[22]**. While Co remains the dominant binder due to excellent wettability, its instability in corrosive or high-temperature environments has driven the exploration of Ni-, Fe-, and alloy-based alternatives. Li et al. **[23]** demonstrated that partially substituting Co with Ni and Fe can maintain the interfacial bonding energy of WC/binder phases, with W-Fe bonds further strengthening interfacial stability. Experimental results showed that the porosity of WC/CoNiFe alloys was significantly reduced to 0.78 %, with a more uniform hardness distribution.

Grain size regulation is another essential strategy. Grain growth inhibitors and rapid densification methods are widely applied to suppress coarsening. At the nanoscale, VC-coated WC core-shell structures effectively reduce grain growth, leading to enhanced hardness and uniformity.

To achieve microstructural refinement and stability, grain growth inhibitors are coupled with rapid densification techniques. For example, WC-VC core-shell architectures form diffusion barriers that suppress grain coarsening and enhance hardness **[24, 25]**. In green remanufacturing, $CaCl_2$-CaO molten salt electrolysis reconstructs nanostructured WC composites while preserving interfacial integrity. Mesoscale tailoring (particle size, binder topology, diffusion barriers) guides crack deflection and toughness **[26]**. In summary, the optimization of cemented carbides should be guided by service requirements and constructed within a four-dimensional synergistic framework involving hard phase selection, binder chemistry, interfacial regulation, and hierarchical grain/topological control. Coordinated modulation of composition and microstructure

enables a tunable balance among hardness, toughness, wear/corrosion resistance, and thermal shock stability **[27]**. This composition-microstructure-property-service chain provides a systematic roadmap for process optimization and performance-oriented design.

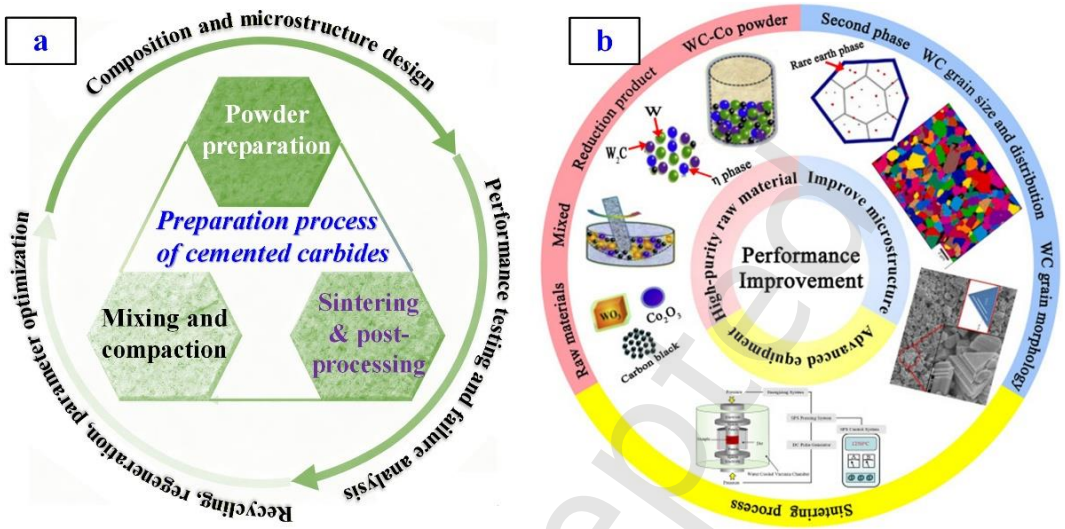

Fig.5 (a) Schematic diagram of the preparation and closed-loop optimization of cemented carbide. The inner hexagons represent the key preparation steps, while the outer cycle illustrates the design-verification-feedback loop for process optimization, and (b) Methods of improving the comprehensive performance of WC-Co cemented carbide (adapted from Ref. **[28]**)

2.3 Fabrication Processes of Cemented Carbides

The fabrication of cemented carbides underpins their mechanical performance and microstructural uniformity (as shown in **Fig.5 (a)**). The typical process includes powder preparation, mixing/ball milling, forming, and sintering densification. Process parameters govern porosity, hard phase grain size (d), binder phase mean free path (λ), hard phase contiguity (C), and interfacial metallurgical characteristics, thereby determining the final microstructure and service reliability (see **Table.2**). Consequently, developing efficient, stable, and controllable fabrication routes remains a central focus in current research and engineering applications (as shown in **Fig.5 (b)**).

Table.2 Key process stages, parameters, and technical objectives for cemented carbide fabrication

Process Stage	Key Procedures	Critical Parameters	Technical Objectives
Powder Preparation	Select high-purity WC powders and binder powders (e.g., Co/Ni) with suitable particle sizes.	WC particle size, purity not less than 99.9%.	Obtain high-purity, fine-grained raw materials to ensure microstructural uniformity.
Mixing and Blending	Mix hard phase and binder phase according to designed ratios, assisted by dispersants.	Hard phase: binder ratio = 85:15 (or optimized proportion).	Ensure compositional uniformity and prevent segregation.
Ball Milling	Use ball-milling media to promote homogeneous dispersion and prevent agglomeration.	Milling time (12-48 h), rotation speed (200-400 rpm).	Achieve uniform particle distribution and microstructural refinement.
Drying and Sieving	Control drying temperature and duration to obtain flowable powders with good dispersibility.	Temperature (80-120℃), sieve size (80-200 mesh).	Improve powder flowability, enhance green compact density, and reduce porosity.
Press Forming	Form green compacts using uniaxial or isostatic pressing methods.	Pressure (100-300 MPa), holding time.	Produce dense and uniform green compacts for subsequent sintering.
Debinding	Remove organic binders slowly in a protective atmosphere.	Heating rate 1 less than ℃/min, temperature (300-600 ℃).	Avoid carbon residue and ensure powder purity.
Vacuum Sintering	Sinter under vacuum or inert gas atmosphere to achieve densification and uniform structure.	Sintering temperature (1350-1500 ℃), holding time.	Obtain high densification and uniform microstructure distribution.
Hot Isostatic Pressing (HIP)	Apply high temperature and isostatic pressure to eliminate residual pores after sintering.	Pressure (100-200 MPa), temperature (1100-1400 ℃).	Further enhance strength and toughness, and eliminate residual porosity.

At the powder stage, it is essential that the hard phase (WC, TiC, TaC, etc.) and the binder phase (Co, Ni, etc.) exhibit high purity, narrow particle size distribution, good sphericity, and strictly controlled oxygen content and specific surface area, which contribute to reducing sintering activation energy and preventing oxidation **[28]**. Hard carbides are generally synthesized via vapor or carbothermal reduction, while binder metals are obtained by electrolysis or atomization. Powder pre-treatment and storage in an inert atmosphere are necessary to prevent agglomeration and contamination,

enabling subsequent uniform dispersion and densification **[29]**.

Ball milling is a key step for homogenizing powder mixtures, promoting pre-alloying, and refining grains. High-energy or planetary milling is commonly conducted in inert or liquid environments, with milling time, rotational speed, and ball-to-powder ratio adjusted according to initial particle size and target microstructure. WC-Co alloy balls are typically used to avoid carbide fracture and cross-contamination, while grain growth inhibitors and dispersants are incorporated to suppress abnormal coarsening and agglomeration, thereby ensuring a stable chemical environment for interfacial metallurgical bonding.

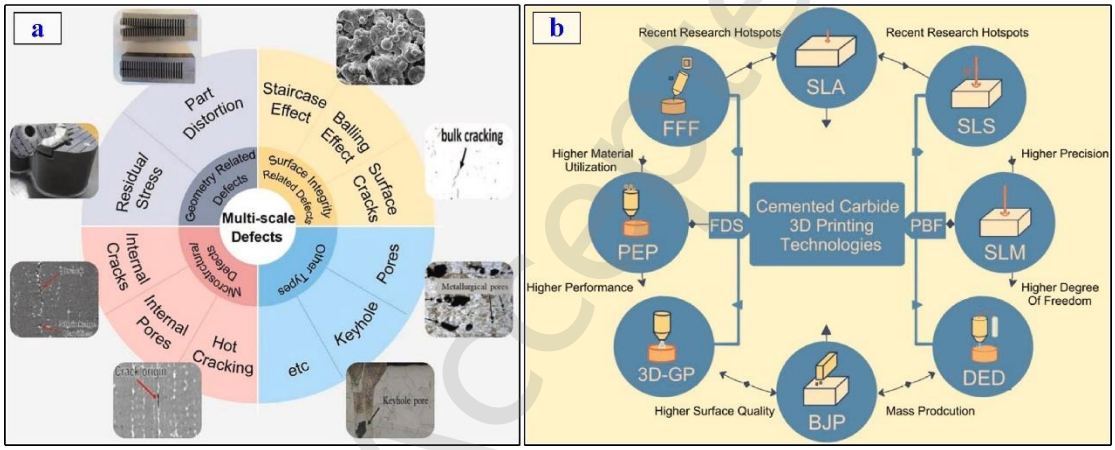

Fig.6 (a) Possible multi-scale defects in cemented carbides 3D printing. Reproduced from Refs, and (b) cemented carbides 3D-printing technologies (adapted from Ref. **[33]**).

The powder forming method directly determines the density and geometric precision of cemented carbide green compacts, and its technological evolution clearly reflects the demand-driven development of industrial applications toward complex components, environmental friendliness, and microstructural performance optimization. Early studies primarily focused on green forming processes. Rose et al. **[30]** proposed a water-based gelcasting combined with rapid prototyping (RPGC) process, in which the introduction of a non-toxic Isobam binder together with grain growth inhibitors enabled the fabrication of WC-10Co components with high density and excellent mechanical properties, thereby validating the feasibility of green forming techniques in improving both environmental safety and mechanical reliability. With the growing demand for

geometrically complex components, 3D printing and additive manufacturing has gradually become an important development direction for cemented carbide forming (as shown in **Fig.6**). Chen et al. **[31]** systematically reviewed two process routes: powder bed fusion (PBF) and forming-debinding-sintering (FDS). They highlighted that PBF urgently requires solutions for crack prevention and porosity control, whereas FDS, owing to its compatibility with powder metallurgy, demonstrates strong potential for producing high-performance components.

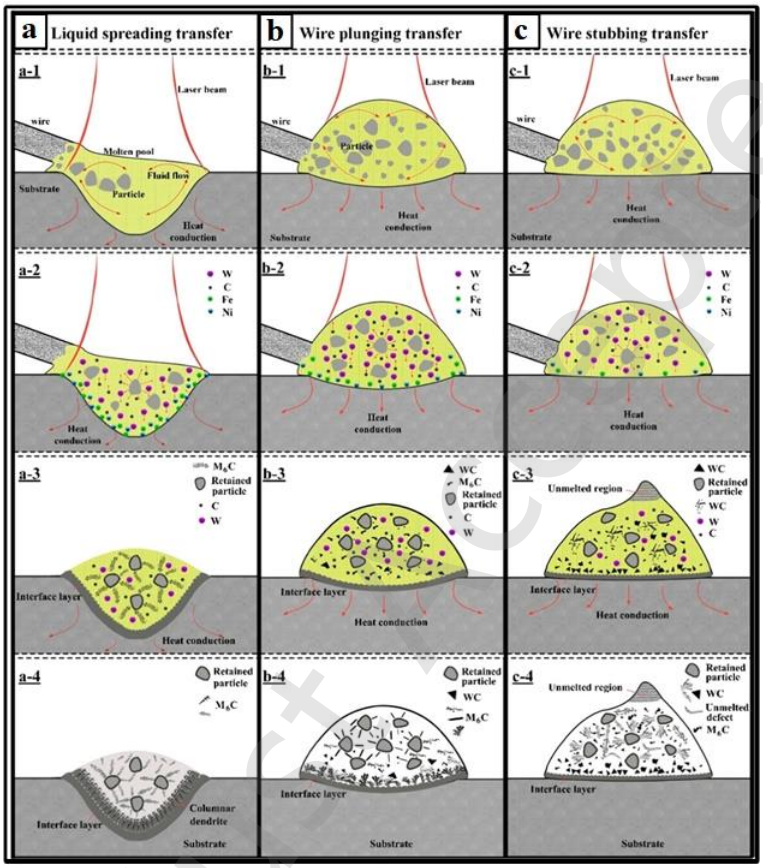

Fig.7 Schematic diagram for showing the microstructure of Ni/WC composite coatings with various wire transfer modes, (a) liquid spreading transfer, (b) wire plunging transfer, and (c) wire stubbing transfer (adapted from Ref. **[36]**).

In practical applications, Miranda et al. **[32]** employed laser powder bed fusion (L-PBF) to fabricate WC-Co and NbC-based cemented carbides, revealing the decisive influence of laser power and scanning speed on microstructural features and defect distribution. They further emphasized the application potential of NbC-based materials in terms of resource substitution and corrosion resistance. Ma et al. **[33, 34]** and Slobodyan et al. **[35]** pointed out that powder engineering parameters (purity, particle size distribution,

and sphericity) are critical for achieving high density and dimensional precision. Meanwhile, the residual stresses and microstructural heterogeneity that are difficult to avoid during laser or electron-beam additive manufacturing must be regulated through functionally graded structural design and numerical simulation approaches. Meanwhile, Zhao et al. **[36]** emphasized the application potential of laser additive manufacturing in carbide-based composites such as WC, TiC, and NbC, particularly highlighting its remarkable advantages in wear resistance, high-temperature performance, and the construction of functionally graded structures (as shown in **Fig.7**). However, the formation of non-equilibrium phases and porosity defects caused by rapid solidification remains a critical bottleneck limiting its engineering applications. In summary, the forming technologies of cemented carbides have gradually evolved from traditional powder metallurgy to green processing and laser additive manufacturing, exhibiting clear trends toward environmental friendliness, structural complexity, and high performance.

Sintering and post-densification are essential for powder densification, microstructural evolution, and mechanical integration **[37]**. Conventional processes mainly adopt vacuum or hydrogen atmosphere sintering at 1350-1500 ℃, with carbon potential strictly controlled to prevent η-phase generation or graphite precipitation, while thermal cycling is employed to mitigate residual stresses and dimensional distortion. Current research has evolved from suppressing macroscopic defects toward microstructure optimization and interfacial regulation, forming a hierarchical process framework.

In the post-sintering machining stage, residual stress prediction models combined with nanofluid minimum quantity lubrication (NMQL) effectively suppress grinding-induced thermal damage and convert surface tensile stresses to compressive stresses, enhancing substrate integrity and coating adhesion **[38]**. Subsequently, laser surface treatment has emerged as a key reinforcement technique. **Fig.8** illustrates the schematic configuration of the laser machining system for cemented carbides, which serves as a conceptual basis for understanding current advancements in laser-based manufacturing technologies **[39]**. Moreover, laser-induced micro-texturing demonstrates strong coupling with functional coatings, where micro-textures refine AlCrN coating

microstructures, increasing hardness and reducing friction, thus enabling integrated surface modification and coating deposition **[40]**.

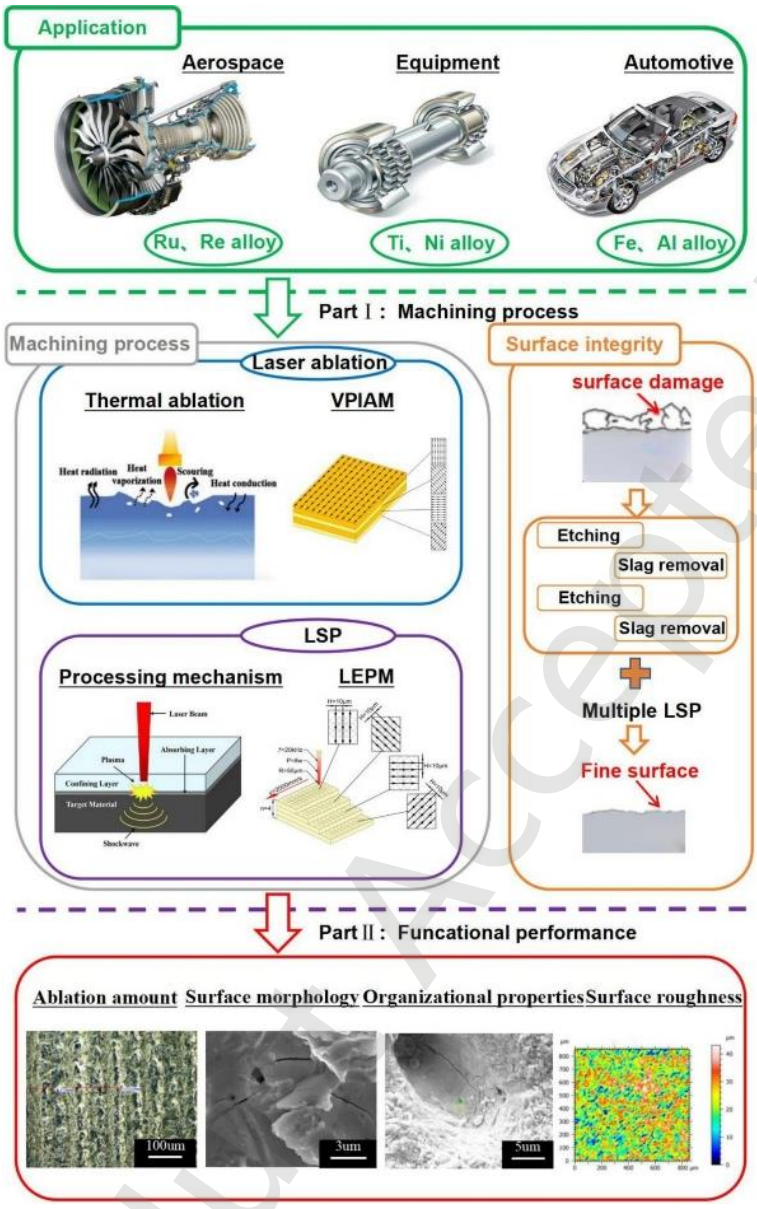

Fig.8 The laser machining process system for cemented carbide (adapted from Ref. **[39]**).

In terms of post-treatment, hybrid processes such as brush polishing and elastic sandblasting effectively optimize surface morphology, improve anti-adhesion properties of PVD coatings, and extend tool life under stable machining conditions **[41]**. Meanwhile, coating systems have been further optimized, arc ion plating-derived AlTiN composite coatings show stronger interfacial adhesion and improved wear resistance, contributing to longer service durations **[42]**. Furthermore, Yan et al. **[43]**

reported that laser texturing of WC-Co substrates combined with CVD diamond films produces wavy interfacial structures that enhance bonding strength, reduce friction, and improve wear resistance, underscoring the importance of interfacial engineering under high-load, long-service conditions.

Table.3 Typical extreme service conditions of cemented carbides and associated tribological issues

Extreme service condition	**Tribological mechanisms**	**Failure features**	**Design considerations**
High-temperature, thermal-oxidative	Adhesive wear, oxidative wear, thermal fatigue	Binder softening, interfacial oxidation, crack propagation	Binder thermal stability, oxidation-resistant composition, microstructural stability
Corrosive, wear-corrosive	Corrosion-wear synergy, electrochemical dissolution	Binder dissolution, interface degradation, wear acceleration	Corrosion-resistant binder, interface stability, surface protection
High contact stress	Fatigue wear, impact damage	Microcrack initiation, fatigue spalling	Strength-toughness balance, crack-arresting design, gradient structures
Erosive/slurry wear	Erosion, abrasive wear	Hard-phase damage, third-body instability	Hard-phase size control, erosion-resistant surfaces
Multi-field coupling	Wear-corrosion-fatigue coupling	Time-dependent degradation, path-dependent failure	Multiscale design, coupled testing and modeling

Overall, cemented carbide fabrication requires balancing mechanical performance, microstructural uniformity, and cost efficiency. Future developments are expected to progress toward greener, smarter, and more efficient approaches, including low-energy green sintering, intelligent process control, multi-field coupled fabrication, and functionally graded material design via additive manufacturing. However, the practical effectiveness of these strategies must ultimately be assessed under extreme service conditions, as material performances are controlled by different tribological degradation mechanisms in different environments. To clarify this engineering context, the typical extreme service conditions of cemented carbides and their associated tribological challenges are summarized in **Table.3**.

3. Tribological Behavior of Cemented Carbides under Typical Non-Corrosive Wear Mechanisms

In non-corrosive environments, the tribological behavior of cemented carbides is primarily governed by mechanical loading, with contact stress, relative sliding, and cyclic loading being the key influencing factors. In the absence of electrochemical corrosion or the involvement of reactive media, the typical non-corrosive wear mechanisms of cemented carbides mainly include adhesive wear, abrasive wear, fatigue wear, oxidative wear, erosive wear, and fretting wear (see **Table.4**). These wear mechanisms not only exhibit distinct material removal modes but also reflect the evolutionary pathways of interfacial damage. At the microscopic level, these wear processes are typically manifested as plastic deformation, crack propagation, oxide film spallation, and particle impact-induced damage. The following sections will respectively examine the interfacial wear characteristics, tribological performance, and microstructural damage mechanisms of cemented carbides under these wear mechanisms.

Table.4 Classification and characteristics of typical non-corrosive wear mechanisms in cemented carbides

Wear Type	Primary Mechanism	Typical Features	Representative service scenario
Adhesive Wear	Surface adhesion and tearing	Groove formation, surface tearing traces	High-speed cutting, dry/boundary lubrication, ultrafine-fine-grained WC-Co (low-medium Co)
Abrasive Wear	Cutting and plowing by particles	Grooves, scratch marks	Drilling/mining, particle-contaminated/slurry contacts, medium-coarse-grained WC-Co (high toughness)
Fatigue Wear	Stress concentration and cyclic fatigue	Surface spalling and fatigue-induced microcracks	Forming dies/forging, cyclic contact loading, binderless WC or low-binder WC-Co (high stiffness)
Oxidative Wear	Oxide film formation and spalling	Brittle oxide layer, oxide debris	High-temperature sliding/machining, oxidizing environment

Fretting Wear	Micro-vibration & localized abrasion	Micro-pits, oxide accumulation	Joints/tooling interfaces, small-amplitude oscillation
Erosive Wear	Impact of high-speed fluid or particles	Erosion pits, material removal	Slurry/particle impingement, high-velocity flow, tough WC-Co (typically coarser grains)

3.1 Adhesive Wear Mechanism

Adhesive wear in cemented carbides under dry sliding or starved lubrication is governed mainly by the binder's propensity for local micro-welding and its shear/thermal stability. The load-transfer capability of the WC skeleton and the integrity of the WC-binder interface further modulate the wear severity. It originates from local micro-welding within the binder phase under high contact stresses. With continued sliding, these junctions are repeatedly sheared, producing transfer-film, localized delamination and spallation. The associated frictional heating softens the binder, facilitates microcrack initiation and propagation along the WC-binder interface, and consequently leads to frictional coefficient fluctuations. The surface-worn features include tearing grooves and material transferring, accompanied by a subsurface deformation layer. During prolonged service, this progressive damage may evolve into severe plastic deformation and ultimately lubrication failure. Fine-/ultrafine-grained WC-Co grades improve hardness and edge retention, yet their propensity for adhesion is governed by binder softening and surface condition. When intermittent impact or severe load fluctuations prevail, toughness-oriented grades (coarser WC or higher Co content) are often selected to suppress chipping, at the cost of reduced hardness and potentially accelerated wear.

Focusing on the adhesive wear mechanism, recent studies have investigated mitigation and regulation approaches from multiple perspectives. Structural control and coating design primarily act by directly suppressing interfacial adhesion and micro-welding behavior. In contrast, predictive modeling, as a general analytical tool applicable to various wear modes, is employed within the adhesive wear research framework to characterize its evolution behavior and critical conditions quantitatively. This approach provides theoretical support for material/coating design and service-condition optimization, thereby indirectly reducing the risk of adhesive wear. Chen et al. **[44]**

demonstrated that nitriding treatment enhances microstructural densification, thereby alleviating adhesive wear through structural control. Zhang et al. **[45]** and Qiao et al. **[46]** introduced MoS_2/PTFE and TiN-WS_2 coatings, respectively, with the latter exhibiting stable anti-adhesion performance at elevated temperatures through soft-hard synergy. Further investigations revealed that the early failure mechanism of coatings is not solely attributed to cumulative wear. Sirtuli et al. **[47]** innovatively proposed that initial notch wear originates from adhesion-induced coating delamination, thereby challenging the conventional understanding. In terms of prediction and modeling, Hao et al. **[48]** developed a multiscale modeling approach that achieved quantitative prediction of adhesive wear, experimentally validated, thus advancing predictive methodologies (as shown in **Fig.9**).

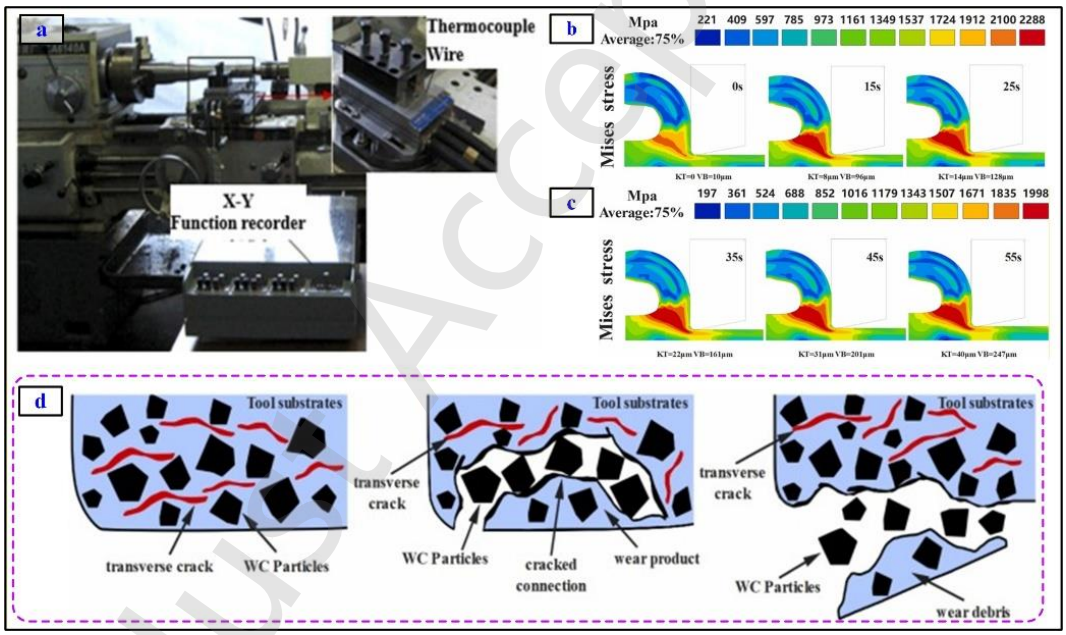

Fig.9 (a) Cutting experimental equipment and measurement system, (b) Tool wear during the previous three iterations, (c) Tool wear during the last three iterations, and (d) Schematic diagram of the flake peeling process (adapted from Ref. **[48]**).

Liu et al. **[49]** proposed a four-stage evolutionary model that systematically summarized the adhesive wear process of cemented carbides. In addition, the counterbody plays a critical role in friction systems. Su et al. **[50]** revealed pronounced adhesive wear phenomena in the frictional interaction between WC-based ceramics and TC4 alloy, and confirmed the effectiveness of graphene nanoplatelet (GNP)

reinforcement (as shown in **Fig.10**). In summary, research on adhesive wear of cemented carbides has gradually evolved into a multi-level framework encompassing "mechanistic elucidation-material modification-predictive modeling" providing both a theoretical foundation and practical pathway for improving service life and designing wear-resistant materials.

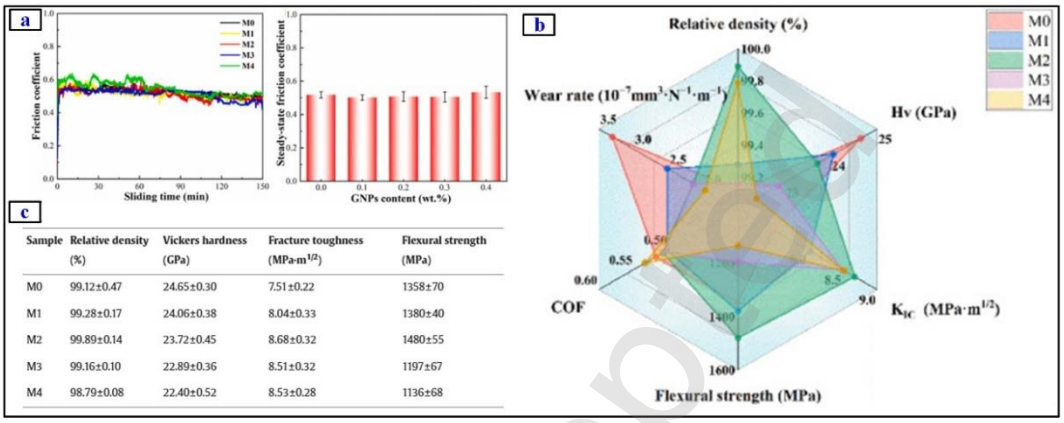

Sample	Relative density (%)	Vickers hardness (GPa)	Fracture toughness (MPa·m$^{1/2}$)	Flexural strength (MPa)
M0	99.12±0.47	24.65±0.30	7.51±0.22	1358±70
M1	99.28±0.17	24.06±0.38	8.04±0.33	1380±40
M2	99.89±0.14	23.72±0.45	8.68±0.32	1480±55
M3	99.16±0.10	22.89±0.36	8.51±0.32	1197±67
M4	98.79±0.08	22.40±0.52	8.53±0.28	1136±68

Fig.10 (a) Friction coefficient of different WC-ZrO_2-Al_2O_3-GNPs ceramics against GCr15 steel ball, (b) Schematic diagram of the relationship between mechanical properties and tribological properties of different WC-ZrO_2-Al_2O_3-GNPs ceramics, and (c) Relative densities and mechanical properties of different samples (adapted from Ref. **[50]**).

3.2 Abrasive Wear Behavior

The introduction of third-body hard particles promotes a mechanistic transition from adhesive wear to abrasion. Once embedded at the interface, these particles induce severe ploughing and micro-cutting of the binder phase, thereby accelerating damage in the adhesive-wear regions and degrading WC-binder interfacial cohesion **[51]**. The worn surfaces are typically characterized by grooves, binder extrusion, and brittle fragmentation of WC grains. Abrasive wear generally results in a higher and less fluctuating coefficient of friction than adhesive wear, and the wear rate is governed by particle hardness, size, and spatial distribution **[52]**. When the particle size markedly exceeds the WC grain size, local stress concentrations can trigger macroscopic spallation, leading to unstable damage propagation **[53]**. Abrasive wear is prevalent in particle-rich environments (e.g., drilling and mining), where entrained sand/cuttings

induce plowing on cemented carbides. Fine-/ultrafine-grained WC-Co grades with high hardness are generally favored to mitigate groove formation. When pronounced impact or load pulsations coexist, medium- to coarse-grained and higher-toughness WC-Co grades are often selected to reduce brittle cracking and spalling, albeit with a potential penalty in abrasive wear resistance due to lowered hardness.

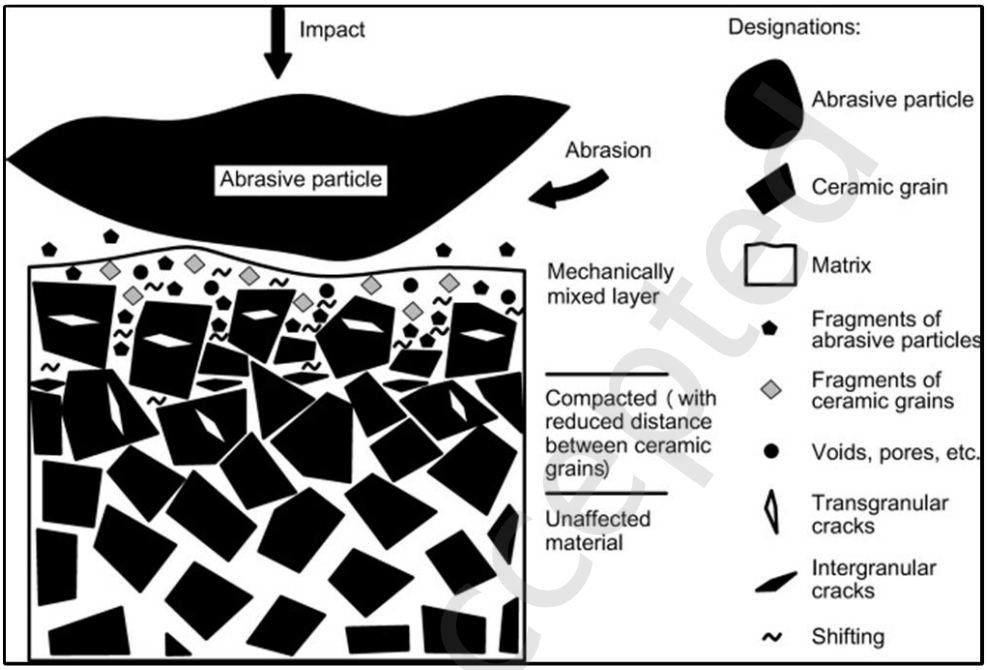

Fig.11 Schematic representation of the surface and subsurface microstructural evolution of cemented carbide under combined impact–abrasion conditions, highlighting the formation of a mechanically mixed layer and compacted zone accompanied by transgranular and intergranular cracking (adapted from Ref. **[57]**).

Studies indicate that abrasive wear mechanisms in cemented carbides have evolved from simple micro-cutting and brittle fracture to multi-coupled processes involving binder removal, interfacial reaction film formation, and surface structural effects **[54]**. Suppression strategies now form a systematic framework integrating process optimization and lubrication control **[55]**, interfacial product regulation **[56]**, microstructural parameter optimization (as shown in **Fig.11**) **[57]**, abrasive characteristic adjustment **[58-60]**, and surface engineering modification **[61]**. Antonov et al. **[57]** developed a wear map based on WC grain size and Co content, revealing that medium grains with 6-8% Co provide optimal resistance under impact-abrasive conditions. Fang et al. **[61]** used laser surface texturing to stabilize lubrication films and

geometry, demonstrating a synergistic pathway between surface engineering and lubrication. Overall, abrasive wear in cemented carbides is primarily driven by third-body particle entrainment that induces plowing and promotes binder removal and WC fragmentation. Accordingly, recent advances focus on multiscale microstructural optimization and surface functionalization, shifting from hardness-oriented strategies to comprehensive anti-wear systems integrating material design, process control, and surface modification.

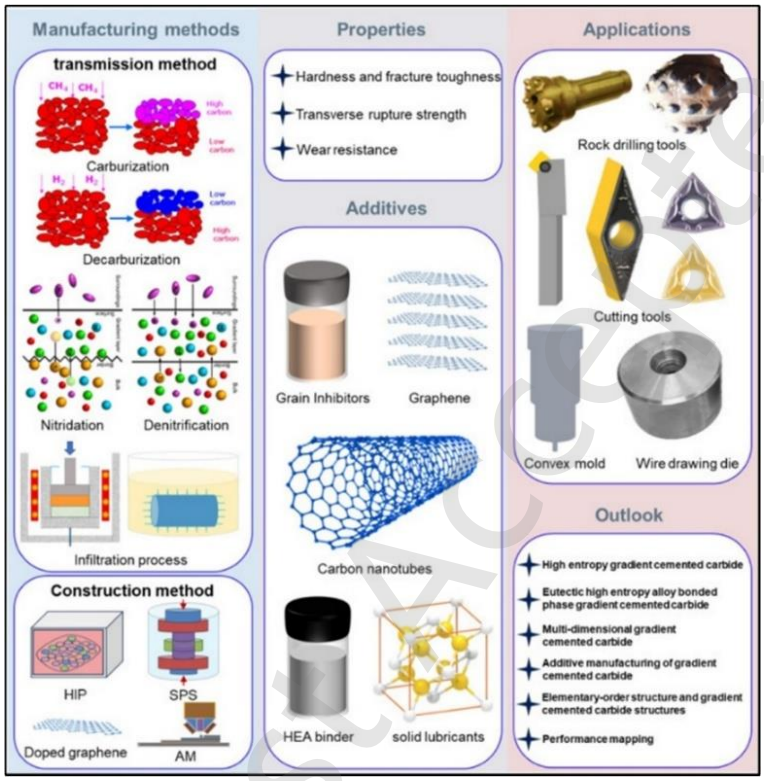

Fig.12 Schematic diagram of manufacturing methods, properties, additives, applications, and development trends of FGCCs (adapted from Ref. **[64]**).

3.3 Fatigue-Induced Wear and Crack Evolution

Following adhesive and abrasive damage, stress concentrations and crack initiation sites develop at the contact interface, facilitating the onset of fatigue wear. Fatigue wear is frequently encountered in intermittent cutting, forming dies, and rolling-sliding contacts, where cyclic contact stresses promote subsurface damage accumulation, crack initiation, and spalling. With increasing sliding cycles, the worn-surface integrity deteriorates, manifested by a gradual increase in the coefficient of friction and subsurface spallation. For cemented carbide components subjected to periodic impacts

(e.g., drill bits and gear contacts), fatigue cracks preferentially nucleate within binder-rich regions or along mechanically weak WC-binder interfaces; the crack path and spall size are further influenced by the WC grain scale and the load-sharing capability of the WC skeleton. Importantly, interfacial susceptibility is governed not only by geometric bonding but also by the binder constitution that provides shear resistance under cyclic loading. Characteristic features include spallation pits and flake-like fracture surfaces. The wear debris predominantly appears as flakes or fragments. Notably, fatigue wear is controlled not only by the magnitude of cyclic loading, but also by the cumulative effects of preceding adhesive and abrasive damage, which are often most pronounced at intermediate loads and sliding speeds.

Recent studies indicate that fatigue wear resistance of cemented carbides is primarily enhanced through microstructural optimization and surface engineering **[62]**. In microstructural optimization, grain refinement and binder phase regulation are key to controlling fatigue crack evolution. Wu et al. **[63]** demonstrated that increasing WC content promotes fine-grained structures and frictional oxide film formation, which suppresses fatigue spallation. Cai et al. **[64]** showed that grain refinement, optimized binder morphology, and solid-solution strengthening improve thermal shock resistance, plastic deformation tolerance, and fatigue wear resistance by enhancing binder work-hardening capacity (as shown in **Fig.12**).

In terms of surface engineering, studies focus on dispersing cyclic stresses and delaying crack initiation via structural design. Tong et al. **[65]** showed that laser micro-texturing traps abrasive particles and attenuates stresses, thereby slowing crack evolution. Zhang et al. **[66]** reported that Cr coatings relieve stresses and shift the failure mode to surface spallation, preventing substrate fatigue cracking. Overall, grain refinement and binder-phase regulation enhance interfacial stability and resistance to crack initiation, whereas coatings and micro-textures can mitigate fatigue wear damage by redistributing contact stresses and promoting a more controlled failure mode **[67]**.

3.4 Oxidative Wear at Elevated Temperatures

Oxidative wear at elevated temperatures is often associated with high-speed dry sliding or starved lubrication and is characterized by repetitive oxide-scale formation, rupture,

and regrowth. From a microstructural perspective, oxidative wear is governed by the load-bearing capacity of the WC skeleton and by the binder phase stability against thermal softening and oxidation. It is further modulated by the WC-binder interfacial integrity, which controls interfacial shear resistance and the stability of the oxide scale. Fine-grained WC-Co grades, often combined with binder modifications, are commonly used to enhance microstructural stability at high temperatures **[68]**. Co/Ni binders preferentially oxidize to CoO/NiO, while WC may form brittle WO_3 at elevated temperatures, resulting in a composite oxide scale. During early wear, the friction coefficient often rises initially and approaches a quasi-steady level as the oxide layer develops. However, once the oxide scale becomes mechanically unstable (e.g., excessive thickening and/or embrittlement), fragmented oxides act as third-body abrasives and promote secondary wear **[69]**. Consequently, worn surfaces exhibit layered spallation, porous oxide accumulation, and oxide-fracture boundaries, which collectively undermine the high-temperature wear stability of cemented carbides **[70, 71]**.

A critical transition occurs around 600 °C, where WO_3 and Co_3O_4 films form on WC/Co surfaces, reducing the friction coefficient from ~0.30 at 200 °C to ~0.05 **[72]**. However, these porous films are prone to spallation, causing increased wear rates despite friction reduction. Microstructural effects show a double-edged role of refinement: nano-WC, due to its high surface area, undergoes accelerated oxidation, with the wear rate at 600 °C approximately four times higher than that of micron-scale WC, and oxygen content increasing to 31.5 wt.% **[73]**. Thus, excessive refinement compromises oxidation resistance, whereas fine grains improve room-temperature wear performance.

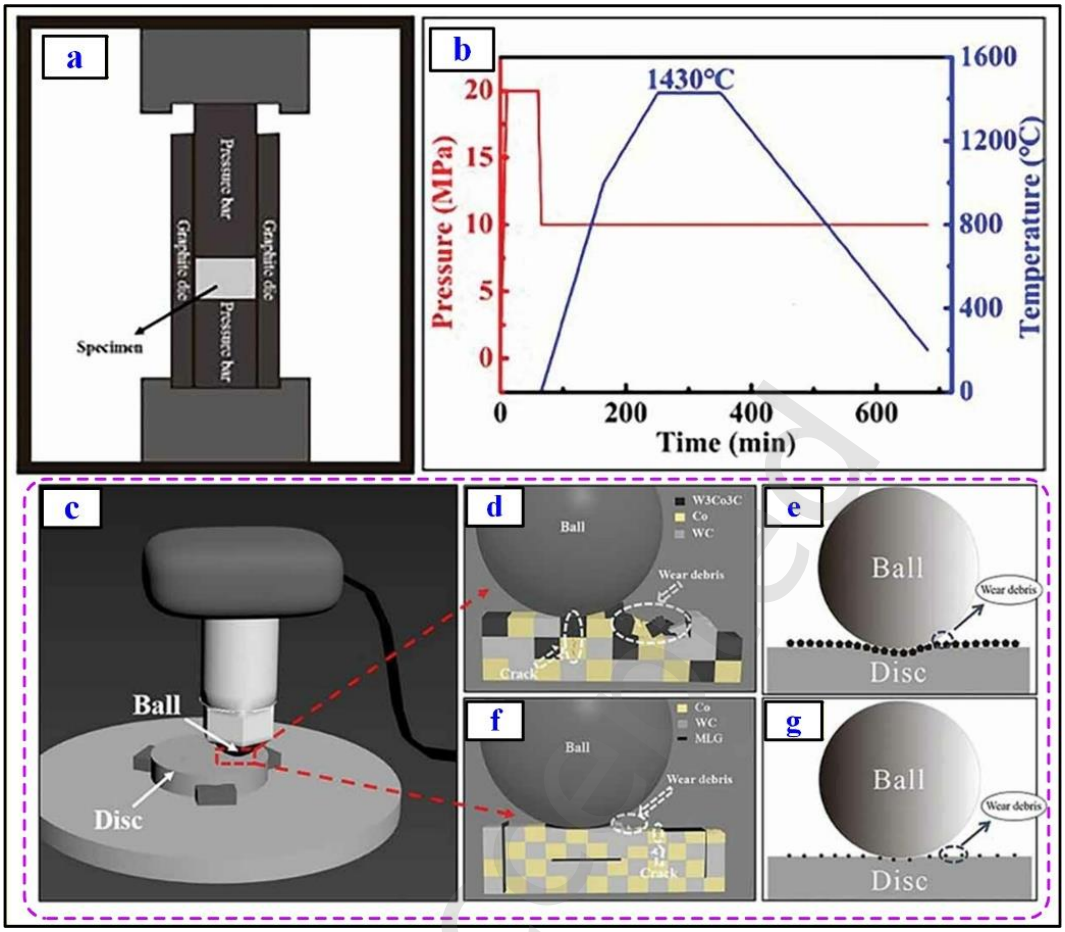

Fig.13 (a) Schematic diagram of the sintering equipment, (b) sintering process curve, (c) Schematic diagram of the friction and wear test device, (d), (e) schematic diagram of friction of the sample with 0 wt% MLG, and (f), (g) schematic diagram of friction of the sample with 0.1 wt% MLG (adapted from Ref. **[75]**).

In practical machining, oxidation often couples with other wear mechanisms, resulting in composite failures. Ultrafine WC-Co tools fabricated via SPS exhibited adhesive-diffusive-oxidative wear when dry-cutting Ti-6Al-4V, yet their service life increased by 1.6-1.8 times compared with YG8 tools **[74]**, indicating that microstructural regulation can partially alleviate oxidation-dominated failure. In terms of material modification, small additions of carbon nanostructures are highly effective. Luo et al. introduced 0.1 wt.% multilayer graphene, suppressing Co embrittlement and achieving a 98% wear volume reduction, with hardness and toughness increasing by 14.5% and 71.8%, respectively **[75]**, demonstrating graphene's potential for enhancing oxidation resistance (as shown in **Fig.13**). Surface engineering provides a more direct strategy:

while multilayer coatings such as TiN/TiCN/Al_2O_3 maintain high-temperature stability, TiSiCN CVD coatings retain high hardness at 900-1100 ℃ and extend tool life by ~30% over TiAlN **[76]**, making them a promising solution for oxidative wear. Overall, existing studies indicate that oxidative wear is strongly temperature-sensitive and microstructure-dependent, and that bulk microstructural tailoring and carbon nanostructure additions have been explored to improve high-temperature performance. In engineering practice, multilayer and composite coatings remain key strategies for enhancing oxide-scale stability.

3.5 Erosive Wear under High-Velocity Particle Impact

Erosive wear arises from the repetitive impingement of solid particles or liquid droplets in high-velocity fluid streams on material surfaces **[77]**. These conditions are typically addressed by medium- to coarse-grained WC-Co grades with enhanced toughness to suppress edge chipping. In the presence of extremely hard particles, hardness is often increased within an acceptable toughness window to improve resistance to micro-cutting. It is characterized by surface pitting, micro-cutting, and thermo-mechanical coupled damage **[78]**. In cemented carbides, the binder phase is often damaged under impact-induced stress concentrations, which can trigger local plastic deformation, binder fracture, and WC particle spallation, producing characteristic erosion pits, radial cracking and fragmented regions. The erosion mechanism is strongly angle-dependent: low impingement angles tend to promote shear-dominated plowing, whereas high angles favor normal indentation and cracking **[79, 80]**. With prolonged exposure, impact-induced defects may facilitate crack growth and accelerate fatigue crack propagation, leading to delamination and granular spallation.

Regarding the erosive wear of cemented carbides, research has developed a complete pathway from mechanistic understanding to design optimization. Current studies emphasize rate-dependent erosion behavior and crack-dominated mechanisms. Bose et al. **[81]** reported that CVD $B_{13}C_2$/WC-Co coatings follow power-law wear (exponent ≈1.2) at velocities of 150–250 m/s, with a critical transition at ~100 m/s. A 13 μm coating outperformed an 18 μm one, highlighting the importance of thickness and interfacial design in crack suppression. Antonov et al. **[82]** showed that fine particle

retention induces stress concentrations, with maximum wear under mixed sand at 80 m/s. In contrast, coarse sand alone promoted a SiO_2 layer covering 70-90% of the surface (vs. 30-50% under mixed sand), with velocity exponents m ≈1.32-1.95, underscoring the key role of third-body effects. Under extreme erosion, Kulu et al. **[83]** proposed design criteria including porosity <3%, compressive residual stress, and dual-binder structures, achieving erosion resistance 10-12 times higher than steel at 30° impact and 2-2.5 times at 90°. Overall, erosive wear studies have gradually shifted from crack-driven damage and spallation toward a multi-mechanism-based interpretation that accounts for third-body particle generation, retention, and re-impingement during repeated impacts. More recent studies increasingly emphasize structure-informed design, where microstructural parameters (e.g., binder-phase stability, carbide grain size, defect population, and interfacial integrity) are tailored to balance hardness with fracture resistance under particle impingement, rather than relying on hardness as a single performance descriptor **[84]**.

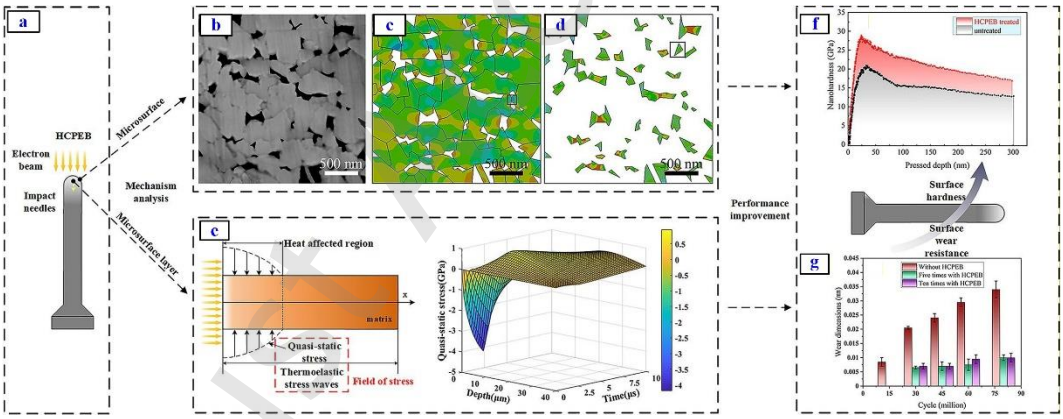

Fig.14 (a) HCPEB treatment of WC-Co impact needle, (b) untreated SEM morphology, (c-d) initial RTS distribution in WC and Co phases, (e) simulated quasi-static stress field, (f) enhanced surface hardness, and (g) improved wear resistance (adapted from Ref. **[87]**).

3.6 Fretting Wear under Micro-Amplitude Vibrations

Fretting wear occurs under conditions where small-amplitude relative displacements (typically less than 100 μm) exist between two contact surfaces, and is commonly observed at interfaces of fastened joints, interference fits, and vibrating structures **[85]**. Microstructurally, fretting wear is governed by the cyclic shear stability of the binder

and the WC-binder interfacial integrity, with interfacial complexion controlling debonding and WC pull-out. This wear mechanism results from coupled effects of mechanically induced abrasion, frictional oxidation, and microcrack accumulation under small-scale sliding. Tribologically, fretting wear typically exhibits an initial sharp rise in friction coefficient followed by stabilization, with surface evolution characterized by cyclic "oxidation-spallation-reoxidation". Typical morphologies include annular oxide zones, crack propagation bands, and fatigue lamellar spallation. Selective binder damage and WC particle interfacial disintegration are distinctive features of fretting wear. A medium-grained WC-Co grade with a balanced hardness-toughness is preferred to suppress crack nucleation and delamination while limiting third-body abrasion.

Research on fretting wear of cemented carbides primarily focuses on surface modification, surface state regulation, and compositional optimization, forming a systematic pathway from microstructural control to service performance enhancement **[86]**. In surface modification, high-current pulsed electron beam (HCPEB) treatment refines WC grains to ~0.1 μm, redistributes residual stress to -506 MPa, and enhances hardness by 39%, resulting in a 71.4% reduction in wear volume (as shown in **Fig.14**) **[87]**. In terms of surface state regulation, interfacial friction conditions strongly affect fretting behavior. Grinding reduces the friction coefficient by ~7.3% and wear volume by 18% **[88]**, while increasing counterbody roughness decreases wear volume by an order of magnitude **[89]**, highlighting the importance of counter-surface morphology. For compositional optimization, introducing composite reinforcing phases effectively enhances performance. $MoSi_2$ addition stabilizes the specific wear rate of TiB_2-based ceramics at ~10^{-6} $mm^3/N{\cdot}m$ **[90]**, and incorporating 6 wt.% Mo_2C into Ti(C,N)-based ceramics increases hardness to 17.86 GPa and toughness to 7.27 $MPa{\cdot}m^{1/2}$, while reducing the friction coefficient and wear rate to 0.49 and 0.9×10^{-6} $mm^3/N{\cdot}m$ **[91]**. Overall, studies on fretting wear of cemented carbides increasingly emphasize integrated strategies that combine surface modification, surface-state control, and compositional design. These approaches aim to refine near-surface microstructures, improve fretting resistance, and maintain an acceptable strength-toughness balance,

thereby providing mechanistic guidance for more reliable service under demanding conditions.

3.7 Coupled wear-mechanism interactions under non-corrosive conditions

Under non-corrosive service conditions, the wear of cemented carbides typically involves the characteristics of multi-mechanism parallelism and dominant mechanism transformation. Any single wear mechanism is usually only suitable for short-term or narrow working conditions. As friction proceeds, coupled feedback may be formed among the interfacial shear instability, the third-body generation and the entrainment of wear debris, which together affect the evolution process of the tribological properties. Accordingly, the typical wear mechanisms such as adhesion, abrasive, fatigue, oxidation, erosion and fretting should be treated as mechanistic constituents of an integrated tribological process, rather than the independent failure modes under complex conditions.

The most representative coupling path is the transition from adhesive wear to abrasion driven by adhesive-derived debris. During the initial adhesive regime, local micro-welding within the binder phase and its periodic shear rupture dominates the interfacial damage, giving rise to a transfer layer accompanied by tearing grooves and localized spallation. Subsequently, the wear debris and the broken WC particles together become entrained and retained within the contact, forming a third-body layer. Consequently, the prevailing damage mode progressively shifts from adhesive shear instability to abrasion-controlled material removal, characterized by ploughing and micro-cutting. Consistent with this transition, the surface morphologies evolve from spallation/tearing features to well-defined furrows and grooves. Moreover, as the third-body shear and the real contact state tend to be dynamically balanced, the friction coefficient tends to evolve from large fluctuations to a relatively stable level, whereas the wear rate may increase due to intensified abrasive action.

Under higher load, severe cycling, or high-temperature conditions, wear coupling in cemented carbides commonly undergoes two key mechanistic transitions. First, defect-assisted fatigue spalling becomes prominent. The abrasive particles' ploughing and erosion promote microcracks at the friction interface. These cracks subsequently initiate

and propagate under alternating shear stresses, potentially leading to interfacial delamination and spallation. As a result, the wear mechanism shifts from instantaneous material removal to a crack propagation-stripping process. Second, the oxide-derived third-body may be progressively abraded. Although an oxide film can form a low-friction-film, it is prone to break and peel off and induce secondary wear when the film is loose, brittle or thinner than the critical stable thickness, forming a friction-wear decoupling phenomenon. In summary, considering the universality of multi-mechanism coexistence and phased transformation under practical operating conditions, it is necessary to complement "single-mechanism" descriptions of non-corrosive wear in cemented carbides with a coupling-transition perspective. This integrated view improves the interpretability of wear evolution and broadens the applicability of mechanistic conclusions across varying regimes.

4. Corrosion-Wear Performance of Cemented Carbides

4.1 Characteristics of Corrosion-Wear

Corrosion-wear is a non-equilibrium process driven by coupled mechanical removal and electrochemical reactions, characterized by cyclic passivation film formation, rupture, and reformation accompanied by material loss. In cemented carbides, degradation is dominated by strong mechanical-electrochemical synergy. The potential difference between hard and binder phases induces micro-galvanic cells, causing selective binder dissolution, weakened interfacial bonding, and carbide pull-out. Concurrently, a third-body layer formed by oxides and corrosion products evolves under shear, regulating frictional response and stress distribution. Under the coupling of frictional heating, corrosion, and fluid shear, nonlinear interfacial responses arise, typically leading to grain boundary disintegration, lamellar spallation, and plowing-induced damage.

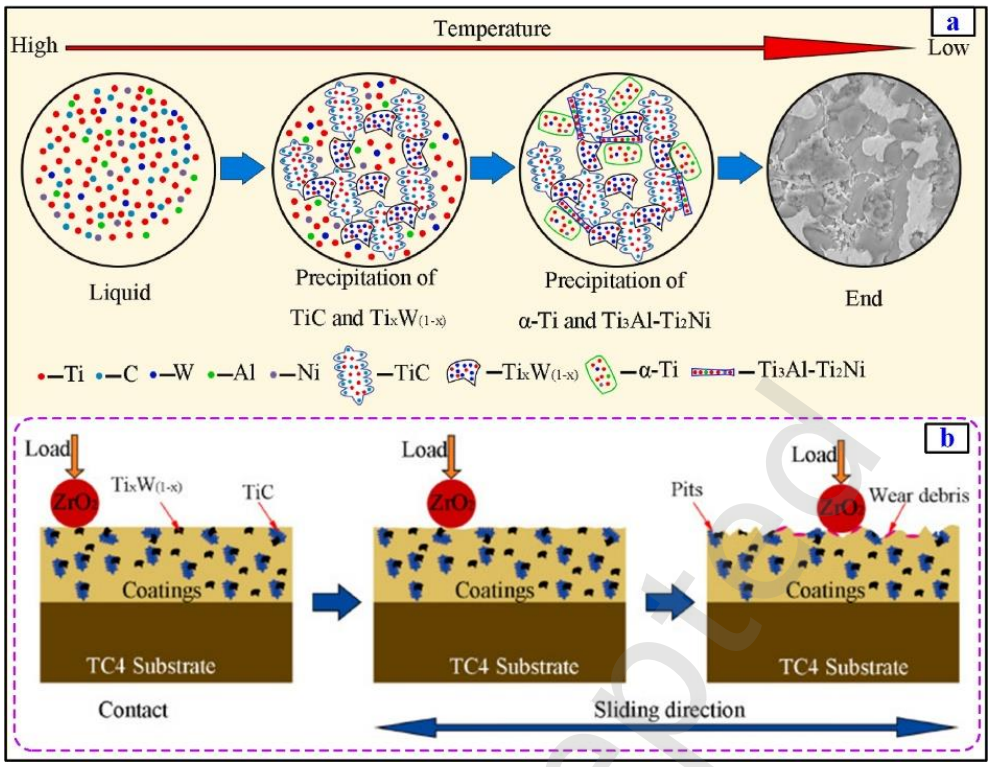

Fig.15 (a) Schematic of metallurgical process of the composite coatings during the cooling process, and (b) The schematic of wear process of prepared composite coatings (adapted from Ref. **[94]**).

Recent advances have clarified corrosion-wear mechanisms of cemented carbides and improved performance. Studies indicate that enhancing wear and corrosion resistance requires both carbide dispersion strengthening and high electrochemical stability of coating interfaces, as well as strong binder-carbide bonding. Zhan et al. **[92]** fabricated Ni60-based TiC/NbC composite coatings via laser cladding and showed that NbC-induced lattice distortion and dispersed carbide phases increased hardness to 981-1045 HV and reduced wear rate to $1.31\times10^{-5}mm^3\cdot N^{-1}\cdot m^{-1}$. Additionally, a stable passive film formed in 3.5 wt.% NaCl reduced corrosion current density to 1.73×10^{-6} $A\cdot cm^{-2}$, demonstrating excellent synergistic wear-corrosion resistance.

Fan et al. **[93]** deposited WC/TiC/Ni coatings on Ti-6Al-4V, achieving a hardness of ~830 HV (2.44× higher than the substrate) and reducing the wear rate by ~36%. Nevertheless, pitting and galvanic corrosion persisted in acidic environments, indicating that interfacial potential differences dominate local failure. To enhance binder-carbide interfacial integrity. Petrosyan et al. **[94]** introduced a rhenium layer via

thermal diffusion, forming a continuous solid solution with Co. This significantly improved interfacial bonding, decreased carbide content in wear debris by 2.0-2.4 times, and effectively mitigated particle pull-out and grain boundary degradation (as shown in **Fig.15**). Recent studies have elucidated the coupled mechanisms of passive film evolution and interfacial degradation in corrosion-wear of cemented carbides through carbide synergistic strengthening, potential regulation, and interfacial solid-solution reinforcement, thereby guiding the design of high-stability coating systems **[95]**.

4.2 Influence of Corrosive Media on the Tribological Performance of Cemented Carbides

The chemical characteristics of corrosive media critically govern the failure rate and dominant wear mechanisms of cemented carbides under friction. Ion species, pH, dissolved oxygen, temperature, and flow velocity modulate the competition between de-passivation and re-passivation, increasing friction coefficient and volumetric wear. Strong Cl^- adsorption facilitates pit initiation and hinders re-passivation, while competitive SO_4^{2-}/Cl^- adsorption alters passive film compactness and defect density, affecting interfacial stability. In neutral to weakly alkaline environments, dissolved oxygen accelerates cathodic reduction and enhances anodic dissolution, whereas increased acidity intensifies binder phase leaching. Elevated temperature promotes ion diffusion and interfacial reaction kinetics, leading to frequent film dissolution/regeneration and thermal stress accumulation due to mismatched expansion coefficients, ultimately causing cracking and spallation. High flow velocity intensifies interfacial shear and mass transfer, thereby inducing flow-accelerated corrosion (FAC), especially when coupled with erosive effects. The presence of suspended particles transforms third-body layers from protective oxide films into abrasive debris, significantly increasing material removal and synergistic wear. Consequently, wear failure in corrosive environments is closely associated with passive film compactness and electrochemical stability, and studies indicate that optimizing coating architecture and re-passivation kinetics markedly improves corrosion-wear resistance **[96]**.

TiAlVN coatings deposited at 0.6 Pa formed a fine-grained dense structure, reducing the self-corrosion current density from 223.8 $\mu A \cdot cm^{-2}$ to 6.16 $\mu A \cdot cm^{-2}$, increasing the

polarization resistance to 1592 Ω, and lowering the wear rate by 2.5 times, indicating that the composite oxide film effectively suppresses Cl^- attack **[97]**. Among complex multi-ion, multiphase, and fluid systems, natural seawater is the most representative coupled environment due to its high Cl^- concentration, elevated dissolved oxygen, and continuous flow **[98]**. Therefore, elucidating the synergistic effects of galvanic amplification, passive film destabilization, and flow-particle interactions under seawater conditions is crucial for identifying dominant failure mechanisms in engineering applications **[99]**.

4.3 Influence of Seawater Environment on the Wear-corrosion Performance of Cemented Carbides

Natural seawater (~3.5 wt.% salinity, pH≈8.0-8.3, containing Cl^-, SO_4^{2-}, Mg^{2+}/Ca^{2+}, enriched in dissolved oxygen, and exhibiting fluidity) represents both the typical and complex wear-corrosion environment for cemented carbides. Its high Cl^- concentration, dissolved oxygen, and flow conditions significantly accelerate the corrosion-wear process of cemented carbides. The main characteristics can be summarized as follows:

4.3.1 Selective Dissolution and Galvanic Driving

In seawater, the failure of WC-based cemented carbides is predominantly driven by selective binder dissolution and galvanic effects from micro-cells. The chemical compatibility of the friction pair critically determines tribological performance: pairing with tin bronze yields an ultralow friction coefficient of 0.02-0.03, whereas 316L stainless steel or TC4 alloy induces rapid failure due to transfer film formation **[100]**. Binder phase modification studies indicate that substituting Ni for Co effectively reduces galvanic coupling, WC-6Ni exhibits a lower friction coefficient (0.17-0.20) and shallower wear tracks compared to WC-6Co in seawater **[101]**. Further alloying with Cr and Mo significantly improves corrosion resistance: relative to WC-Co, the open-circuit potential shifts positively by ~400 mV, the corrosion current density decreases by an order of magnitude, and the charge transfer resistance increases to 10^6 Ω·cm^2. At ~0.6 wt.% Mo, pitting inhibition is most pronounced, demonstrating that Ni-Cr-Mo binders can form stable passive films and markedly enhance corrosion resistance **[102]**. Engineering lifetime tests corroborate these mechanisms.

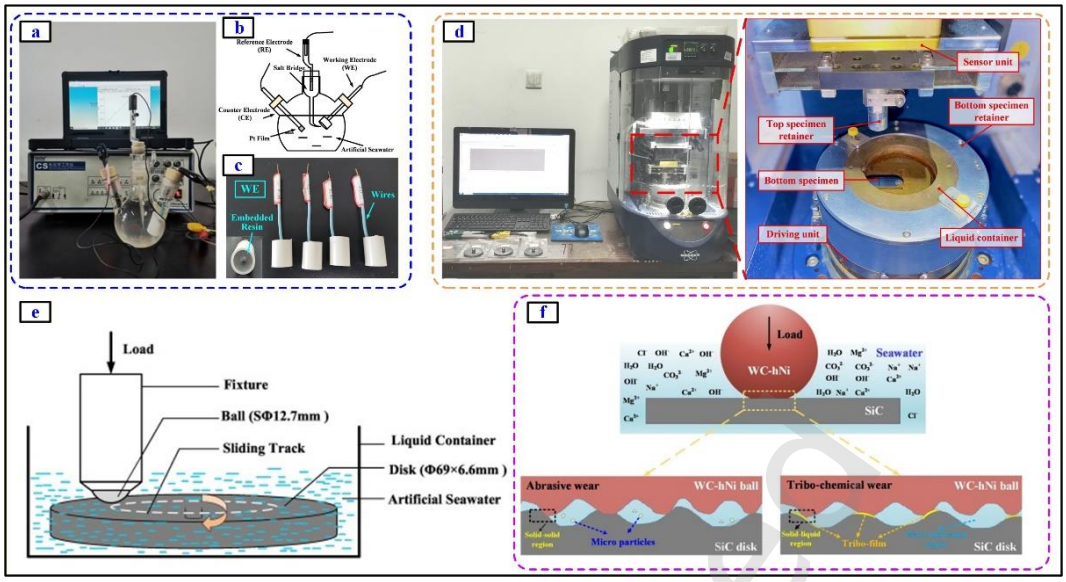

Fig.16 (a) electrochemical workstation, (b) standard three-electrode device, (c) working electrode, (d) UMT TirboLab friction and wear tester, (e) Principle of experimental structure, and (f) Schematic of the wear mechanism of the WC-hNi/SiC tribopair in seawater (adapted from Ref. **[104]**).

For example, WC-8Co exhibits an ultralow friction coefficient (0.01-0.02) in self-mated pairs under artificial seawater, however, the wear rate of the stationary ring is approximately three times higher than that of the rotating ring, attributed to particle pull-out and plowing wear induced by Co dissolution **[103]**, indicating strong dependence on binder composition. Subsequent studies identified a Ni-content window effect: WC-9Ni exhibited optimal corrosion resistance in seawater, with an icorr of 7.27×10^{-7} A·cm^{-2} and a corrosion rate of 0.0046 mm·a^{-1}, whereas deviations from this composition resulted in significant performance degradation (as shown in **Fig.16**) **[104]**. In coating systems, high-entropy alloy (CoCrFeNi) binders increased E_corr to -230 mV and reduced icorr to 1.3 μA·cm^{-2} **[105]**. Likewise, Fe-based amorphous composite coatings, leveraging dense amorphous structures and multi-element alloying, reduced corrosion current by approximately an order of magnitude and exhibited no pitting **[106]**. Overall, counterbody selection, binder phase optimization, alloying regulation, and advanced coating design collectively suppress galvanic effects and selective dissolution in seawater, providing systematic strategies for the long-term durability of WC-based cemented carbides.

4.3.2 Film Embrittlement and Rapid Renewal

In seawater wear-corrosion environments, coating embrittlement and rapid renewal mechanisms have become key research priorities **[107,108]**. Recent findings indicate a shift from isolated enhancement of corrosion or wear resistance toward an integrated optimization strategy of "structural densification-interfacial stabilization-self-healing" **[109,110]**. For instance, multilayer chromium coatings suppress Cl^- penetration through crack-arresting and stress-relief mechanisms, exhibiting excellent crack passivation and re-passivation capabilities. These films achieved a corrosion current density as low as 6.65×10^{-7} $A\cdot cm^{-2}$ and a wear rate reduced to 3.48×10^{-5} $mm^3\cdot N^{-1}\cdot m^{-1}$ **[111]**.

PVD TiCN coatings, characterized by a high hardness of 31.6 GPa and a non-columnar microstructure, achieved an ultralow wear rate of 1.07×10^{-6} $mm^3\cdot N^{-1}\cdot m^{-1}$ in artificial seawater, significantly outperforming TiN and uncoated substrates and demonstrating strong resistance to film embrittlement **[112]**. Overall, recent advances indicate a transition from isolated improvements in corrosion or wear resistance to an integrated optimization strategy of structural densification-interfacial stability-self-healing. Through interfacial stabilization and rapid re-passivation driven by self-healing mechanisms, coatings deliver durable tribo-corrosion protection in seawater environments.

4.3.3 Flow and Erosion-Corrosion Coupling

Although current studies have revealed aspects of flow- and erosion-corrosion coupling in seawater for cemented carbides, a comprehensive mechanistic understanding remains limited. Regarding binder phase effects, the Ni/Co ratio strongly influences erosion-corrosion performance in Ti(C,N)-based cermets: introducing an optimal Co content reduces wear rate from 35.7×10^{-3} mm^3/h to 17.7×10^{-3} mm^3/h, whereas excess Co induces embrittlement and deteriorates performance, underscoring the need to balance hardness and toughness **[113]**. Additionally, impact angle studies show that Mo_2NiB_2-Ni cermets exhibit cutting-dominated wear at low angles and impact-dominated wear at high angles, with the Ni binder phase playing a key role in suppressing crack propagation within the ceramic skeleton (as shown in **Fig. 17**) **[114]**. However, most studies have employed single-impact-angle tests, which do not fully

capture the complexity of real flow fields. Microstructural refinement has been shown to enhance erosion–corrosion resistance significantly. For instance, nanostructured Cr_3C_2-NiCr and WC-based coatings exhibit superior performance due to grain refinement strengthening and rapid re-passivation **[115]**, while Fe/TiC-based coatings maintain stable wear and corrosion resistance in artificial seawater through matrix–reinforcement synergy **[116]**. Overall, binder phase regulation, impact angle effects, and microstructural optimization represent current advancements, yet systematic research on multi-factor coupling mechanisms remains urgently required.

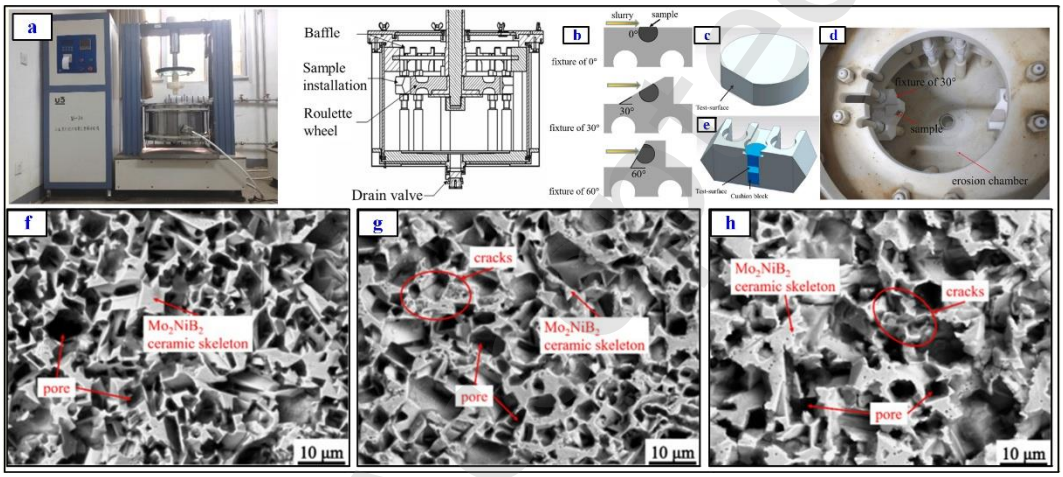

Fig.17 (a) The erosion tester and schematic representation, (b)-(e) The schematic diagram of sample and fixture with different impact angles, and Wear surface of Mo_2NiB_2 ceramic skeleton at 12 h of impact angle: (a) 0°, (b) 30° and (c) 60° (adapted from Ref. **[114]**).

In seawater environments, cemented carbide failure is further influenced by fretting and biological factors in addition to corrosion. Under wave-induced vibration, interference-fit interfaces experience fretting tribo-corrosion characterized by cyclic "oxidation-spallation-reoxidation" during which the binder phase is preferentially degraded, leading to premature localized failure. Meanwhile, biofouling and microbial activity induce interfacial pH fluctuations and release corrosive metabolites (e.g., sulfides), impairing re-passivation and accelerating pitting-type tribo-corrosion. Although current research is limited, these effects may significantly intensify material degradation. Given the high-frequency de-passivation and rapid film renewal in seawater, durability enhancement relies on stabilizing galvanic systems, mitigating thermomechanical film

destabilization, and reducing flow/particle-induced de-passivation. Consequently, systematic investigation of binder alloying, microstructural engineering, and multifunctional coatings is essential for extending service life.

4.4 Corrosion-Wear Resistance Mechanisms of Cemented Carbides

The corrosion-wear resistance of cemented carbides arises from the interplay of de-passivation and re-passivation dynamics, galvanic effects, thermal stress, erosion-corrosion coupling, and corrosion fatigue, which are governed by binder composition, microstructural scale, and surface state. Alloying with Ni-Cr, Fe-Ni-Co, or high-entropy binders improves interfacial electrochemical uniformity and reduces binder dissolution, while reinforcing phases (e.g., VC, Cr_3C_2, TaC) enhance binder strength and mitigate erosion damage. Grain refinement and graded architectures improve thermal conductivity and reduce thermal stress-induced cracking. Pre-alloyed powders, interfacially active elements, and HIP densification strengthen carbide-binder bonding and delay corrosion fatigue crack propagation. Surface texturing improves load capacity, whereas nanostructured or self-healing coatings promote rapid re-passivation, effectively reducing fretting corrosion.

Although compositional, microstructural, and surface-level strategies provide multidimensional optimization pathways, current research lacks quantitative evaluation of the relative contribution and interaction of failure mechanisms under varying service conditions, limiting the establishment of unified failure criteria. In addition, the long-term reliability of cemented carbides under multi-physics coupling and the stability of surface-engineered modifications remain insufficiently validated. Future work should focus on developing cross-scale evaluation frameworks integrating experimental simulation, mechanistic modeling, and service life prediction to achieve a transition from localized protection to holistic steady-state control, thereby ensuring reliable performance in complex marine environments.

5. Surface Strengthening and Protection Strategies for Cemented Carbides

Previous studies indicate that failure of cemented carbides in wear–corrosion-coupled environments primarily stems from uncontrolled microstructural evolution and degradation of surface protective films. Enhancing service stability therefore requires synergistic regulation of multiscale structures and interfacial reactions to construct a strengthening system with high thermodynamic stability and self-passivation capability. Fundamentally, tribology-oriented surface strengthening and protection strategies for cemented carbides are achieved through the coordinated design of hard phases, binder phases, and additives, aiming to regulate interfacial shear behavior, third-body dynamics, and wear mechanisms across multi-scales (see **Table.5**). To further clarify the performance-governing relationships in cemented carbides, **Fig.18** schematically summarizes the surface technologies related to cemented carbides. This chapter addresses surface strengthening and protection strategies for sintered cemented carbides as the substrate, including microstructural tailoring, PVD/CVD coatings, and surface texturing.

Table.5 Tribology-oriented surface strengthening and protection strategies for cemented carbides

Strategy category	**Strengthening approach**	**Key tribological effect**	**Representative systems**	**Tribological benefit**
Microstructural design	Grain refinement & gradient structure	Suppresses abrasive and micro-cutting wear	Submicron/nanocrystalline WC, gradient-grained WC-Co	Improved abrasive wear resistance
Hard-phase design	Multi-carbide solid solution	Reduces carbide pull-out during sliding	WC-TiC-TaC, WC-Ti(C,N)	Enhanced wear and oxidation resistance
Binder-phase optimization	Binder composition control	Stabilizes carbide-binder interface under wear-corrosion	Co-, Ni-, Fe-based binders	Reduced wear-corrosion degradation

Grain-growth inhibition	Grain boundary segregation	Limits third-body debris generation	VC, Cr_3C_2, NbC additives	Improved wear stability
Dispersion strengthening	Nanoparticle dispersion	Resists plastic deformation under sliding	Al_2O_3, SiC, Ti_3SiC_2, TiN/TiCN nanoparticles	Enhanced sliding wear resistance
Alloying modification	Binder alloying	Forms protective tribo-oxide layers	Microalloying with Cr, Mo, W, Y, Ce elements	Mitigated corrosion-assisted wear
Lubrication design	Solid lubricant incorporation	Lowers interfacial shear stress	Graphite, MoS_2, h-BN, graphene-based nanolayers	Reduced friction and wear
Densification processing	Porosity suppression	Reduces contact fatigue damage	SPS, HIP, vacuum sintering	Improved fretting resistance
Gradient or layered structuring	Layered & gradient architecture	Redistributes contact stress	Gradient WC-Co structures	Enhanced wear durability

5.1 Types and Grain Size of Hard Phases

The crystal structure and grain size of hard phases govern baseline hardness, critical wear stress, and thermo-corrosion stability. Optimizing carbide composition and regulating grain size and contiguity enables a balanced hardness-toughness-corrosion resistance profile, providing a stable structural foundation for binder and surface engineering.

WC-based cemented carbides dominate due to high hardness and thermal conductivity but suffer grain coarsening and softening under erosion–corrosion, necessitating multi-component regulation. TiC/Ti(C,N) improves oxidation and diffusion resistance and refines WC lamellae, enhancing low-stress wear resistance, although excessive γ-phase formation may reduce compressive strength under high stress **[117]**. TaC/NbC additions enhance red hardness and chemical stability. Multiphasic systems such as WC-TiC-TaC form thermally stable cubic γ-phases that suppress abnormal grain growth and facilitate passive film formation in oxygen-/chloride-rich environments, reducing third-body fragmentation.

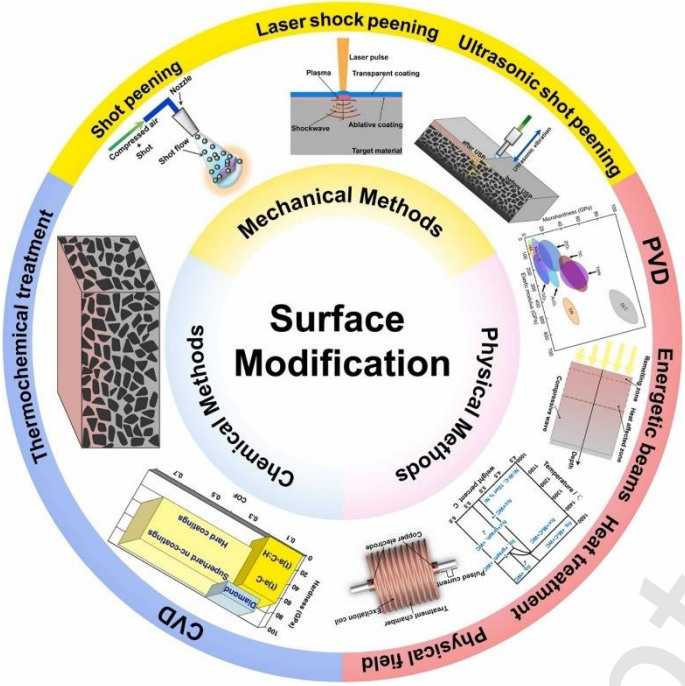

Fig.18 Surface modification technologies for improving tribological properties of cemented carbides (adapted from Ref. **[37]**).

Grain refinement to <1 μm increases hardness and critical cutting stress but elevates interfacial reactivity and brittleness, requiring inhibitors (e.g., VC, Cr_3C_2) and dense sintering (SPS/HIP) **[118]**. Conventional 1-5 μm grains enhance crack deflection under impact and corrosion fatigue. Gradient grain architectures, combining a fine-grained surface with a coarse-grained core, achieve surface anti-plowing resistance and core load-bearing toughness, enabling multiscale performance synergy.

Microstructural connectivity is critical to wear–corrosion synergy. Insufficient WC contiguity and an excessively long binder mean free path reduce load-bearing capacity and intensify localized corrosion. In contrast, a uniform skeleton and controlled phase boundary distribution support continuous third-body layer formation and limit galvanic localization. Nanocrystalline gradient architectures offer a promising alternative to conventional microstructures. Studies indicate that stabilizing WC grain sizes at 149-170 nm with gradient layers of 33-55 μm maintains high hardness (HV ≈ 2200) while improving fracture toughness to 10.5-10.9 $MPa \cdot m^{1/2}$. In Ti alloy cutting, such tools exhibit a wear depth of only 0.096 mm after 1000 m, approximately 35% lower than reference samples **[119]**. Overall, research has progressed from single grain refinement

to multiscale inhibition strategies, with nanocrystalline gradient designs demonstrating high potential for improving both wear and corrosion resistance.

5.2 Composition and Content of the Binder Phase

The binder phase governs interfacial toughening, energy dissipation, and electrochemical stability, regulating the balance between film degradation and re-passivation under wear-corrosion coupling. Tailoring its composition, content, and carbon balance enables optimized hardness-toughness synergy while mitigating chloride-induced dissolution. Co-based binders exhibit good wettability but suffer from high anodic dissolution in Cl^- environments. Ni-based binders form more stable passive films, whereas Fe-Ni-Co binders offer cost-effective performance and can be strengthened via Cr/Mo alloying. High-entropy alloy (HEA) binders provide superior thermal and corrosion stability due to high configurational entropy and sluggish diffusion. Binder volume must balance toughness and hardness: excessive content weakens cutting resistance and film integrity, whereas insufficient content promotes embrittlement. Carbon deficiency induces brittle η-phases, while excess carbon leads to graphite precipitation, disrupting passive film stability. Vacuum/protective sintering and HIP densification reduce porosity and galvanic susceptibility, enhancing long-term durability.

Extensive empirical studies have further revealed the critical role of the binder phase in corrosion-wear behavior. For example, nanoindentation and statistical analyses showed that the intrinsic hardness of Co binder constrained by WC is approximately 8.1 GPa, corresponding to a flow stress of 1.8-2.4 GPa. Moreover, the basal plane hardness of WC was found to be 20-30 % higher than that of the prismatic plane, providing quantitative support for energy-dissipation modeling **[120]**. For Ni-Fe binders, hardness ranges from 4.4 to 8.5 GPa (approximately 170 HV after correction) and increases with decreasing mean free path, indicating that constraint-solid solution effects can enhance their resistance to pitting corrosion **[121]**. Diao et al. employed Ni_3Al as a substitute for Co and introduced 0.3 wt.% SiC_w, achieving a densification of 96.5 %, hardness of 1570 HV, and fracture toughness of 13.1 $MPa \cdot m^{1/2}$ at 1500 °C, with excellent oxidation and chloride resistance **[122]**. The Co-Ni-Fe binder phase enabled low-temperature

densification at 1050 ℃, yielding a hardness of 1781 HV and toughness of 10.52 $MPa \cdot m^{1/2}$, representing a 5-10 % improvement over conventional WC-Co **[123]**. Particularly notable is the CoCrNi multi-principal-element binder phase, which reduced corrosion current density by 70 % and increased polarization resistance by an order of magnitude, attributed to the formation of a Cr_2O_3-NiO-$Ni(OH)_2$ passive film, thereby significantly mitigating galvanic corrosion **[124]**. In summary, research has evolved from conventional binder phase characterization toward compositional tuning, phase structure optimization, and multi-principal-element design, providing new foundations for developing high-strength, tough, and corrosion-resistant cemented carbides.

5.3 Effect of Additives

Additives enhance corrosion–wear resistance by inhibiting grain growth, providing dispersion strengthening, modifying interfaces, and offering solid lubrication. Appropriate selection of type, size, and content stabilizes the third-body layer, accelerates re-passivation, and delays film failure while preserving matrix toughness.

5.3.1 Grain Growth Inhibitors

Grain growth inhibitors such as VC, Cr_3C_2, and NbC pin WC grains during sintering, refine grain size, and purify boundaries, thereby increasing hardness, reducing abrasive penetration, and lowering interfacial corrosion susceptibility. However, excessive addition may form brittle networks or promote η-phase precipitation, reducing fracture toughness. Thus, inhibitor content must be optimized alongside sintering kinetics and carbon potential. First-principles studies show that V, Cr, and Mn segregate at carbon-rich WC/WC interfaces, increasing interfacial separation work and enhancing boundary stability, supporting the atomic-scale mechanism of VC and Cr_3C_2 effects **[125]**. In functionally graded composite ceramics (FGCCs), VC can significantly refine grains and reduce the gradient layer thickness by approximately half, whereas NbC raises the peak transverse fracture strength to 2400 MPa and maintains a high-temperature hardness approximately 100 HV higher than that of conventional samples at 700-800 ℃, demonstrating a combined effect of dissolution/reprecipitation inhibition, grain refinement, and oxidation resistance **[126]**.

5.3.2 Dispersion Strengthening Particles

Nanoscale dispersoids such as Al_2O_3, SiC, or TiN/TiCN enhance binder yield strength and high-temperature softening resistance, thereby mitigating thermal stress-induced coating cracking. Their strengthening efficiency depends on particle size and interfacial wettability, as excessive size or poor wettability may cause agglomeration and debonding, compromising structural stability. Thus, achieving uniform nanoscale dispersion is critical. For example, the addition of 3 wt.% Ti_3SiC_2 forms (W, Ti)C/WSi_2 dispersions and an interfacial (W, Ti)C layer, refining WC grains to ~0.30 μm, and yielding a hardness of 2076 HV and fracture toughness of 10.1 MPa·$m^{1/2}$, attributed to diffusion barrier effects and crack-deflection toughening **[127]**.

5.3.3 Addition of Alloying Elements

The addition of Cr, Mo, W, and rare-earth elements (Y, Ce) enhances binder corrosion resistance and mechanical stability. Cr forms a dense Cr_2O_3 passive film, serving as the primary element for corrosion resistance. Mo suppresses chloride-induced pitting and stabilizes passive films via MoO_4^{2-} formation, while Cr-Mo synergy significantly improves re-passivation in marine environments. W contributes mainly to solid-solution strengthening and high-temperature hardness but has limited impact on passivation. Rare-earth elements (e.g., Y, Ce) purify interfaces, refine inclusions, and improve oxide film adhesion, enhancing integrity and re-passivation kinetics. For instance, Y_2O_3 addition nearly doubles the gradient layer thickness in FGCCs (~2 mm vs. 1 mm), increases strength by ~30%, and reduces cracking and corrosion via Co-phase solid-solution strengthening **[128]**.

5.3.4 Solid Lubricants and Two-Dimensional Materials

Solid lubricants such as graphite, MoS_2, h-BN, and graphene generate a low-shear third-body film, reducing friction at sliding interfaces. Rather than bulk addition-which compromises density and load capacity-a surface/coating composite strategy, incorporating limited lubricating phases in the top layer or forming nanoscale multilayers, enables rapid interface lubrication without sacrificing matrix toughness, achieving a balance between lubrication efficiency and structural integrity.

5.4 Surface coating technology

Surface coating technology provides an effective approach to enhancing the service

stability of cemented carbides under extreme conditions by constructing a functional interface layer on the substrate **[129]**. This engineered interface modulates load transfer, interfacial reactions, and wear evolution within the frictional contact zone. From a tribological perspective, the primary mechanisms involve isolating the substrate from direct participation in interfacial sliding and reducing interfacial shear stress, thereby leading to a lower friction coefficient **[130]**.

PVD/CVD hard coatings, such as TiN, Ti (C, N), TiAlN, AlCrN, effectively suppress ploughing wear owing to their high hardness and excellent high temperature stability, and exhibit relatively stable wear behavior under high-speed cutting and high temperature sliding conditions. Multilayer or gradient structures design can helpful to alleviate the stress concentration arising from thermal-mechanical coupling. However, thermal mismatch and interface defects may still promote coating spalling under high load or cyclic thermal conditions. Meanwhile, low friction carbon-based coatings, such as DLC and ta-C, reduce the friction coefficient by forming a low-shear-strength interface, which is suitable for boundary lubrication conditions. However, due to its high internal stress level, it is usually necessary to combine metallic interlayers or nano-multilayer architectures to improve the adhesion reliability. Consequently, post-treatment processes such as shot peening or surface rolling are often required to stabilize the coating structure and ensure reliable tribological performance **[131]**.

5.5 Surface texturing technology

The surface texture introduces additional degrees of freedom for controlling frictional interfaces by orderly regulating the surface geometry of the cemented carbides, which plays a complementary role in improving the friction-wear behavior **[132]**. From the perspective of tribological mechanisms, micro-/nano-scale textures mainly affect the tribological behavior through contact stress dispersion, entrapment of abrasive particles, and lubrication medium storage. Appropriately designed textures can store wear debris and lubricating medium during wear, suppressing the uncontrolled migration and excessive interfacial shearing within the contact zone **[133]**. As a result, localized stress concentrations are effectively alleviated. Under dry friction or starved lubrication conditions, textures can also alleviate the formation of ploughing grooves and alter the

wear evolution path. The synergistic design of surface textures with coatings or solid lubricants can further amplify their tribological benefits. In such hybrid systems, the texture can be used as the film-forming starting point of the lubricating phase and capture the wear debris, while the coating provides load-bearing support for the textures and forms a low-friction interface **[134]**. The texture-coating synergy contributes to enhanced, more stable tribological behavior under extreme conditions.

5.6 Synergistic tribological design strategy of microstructure control-coating-texture

Table.6 summarizes representative material-/process-level strategies for enhancing the mechanical and tribological performance of cemented carbides through hard phase, binder phase, and additive regulation. Additive systems enable multiscale synergy via atomic-level segregation control, grain refinement and dispersion strengthening, and gradient or layered architectures, thereby suppressing galvanic corrosion, stabilizing the third-body layer, and improving re-passivation **[135]**. The core innovation lies in the integrated optimization of performance and mechanism **[136]**.

Table.6 Summary of material and process strategies for improving mechanical and tribological properties of cemented carbides

Strategy	Mechanism	Specific Measures	Performance Effects
Optimization of Materials & Microstructure	Grain refinement and phase adjustment reduce interfacial stress and crack initiation.	Use submicron WC+VC/Cr_3C_2 inhibitors, introduce TiC/TaC/NbC carbides, optimize binder ratio, sinter via HIP/SPS.	Higher hardness and toughness, suppressed crack propagation, strength-toughness synergy.
Surface Coating Technology	High-hardness/low-friction coatings form protective barrier, lowering shear and corrosion coupling.	Apply PVD/CVD, DLC/ta-C with buffer layers	Reduced friction and wear, improved oxidation and adhesion, longer tool life.
Heat Treatment and Process Optimization	Enhance purity and densification to suppress brittleness and optimize stress.	High-purity powders, HIP/SPS vacuum sintering; peening, process-structure-property control.	Higher strength and fatigue resistance, lower variability, improved reliability.

Overall, the optimization of wear resistance of cemented carbides under extreme

conditions has been controlled by a single material or an individual surface treatment, and has gradually developed into a systematic tribological design framework for the synergistic effect of matrix microstructure, surface coating and surface texture. Within this framework, the matrix microstructure determines the overall load-bearing capacity and damage mode. The surface coating mainly regulates the interfacial reactions and shear behavior. The surface texture further optimizes the interfacial lubrication state. The above multi-level strategies synergistically act on the contact stress distribution, interfacial shear response and wear evolution process to achieve cross-scale regulation from the inside of the material to the friction interface. Nevertheless, there are also potential trade-offs among different strategies. For instance, the increase in hardness may elevate brittleness risk, whereas excessively high texture densities can reduce the effective load-bearing area. Consequently, the design must be combined with specific working conditions to match the loading modes, sliding state, environmental conditions and lifetime requirements. Looking forward, the surface strengthening and protection strategies of cemented carbides will pay more attention to the mechanism-driven collaborative design and service-condition adaptability, thereby achieving the collaborative optimization of wear resistance, corrosion resistance and service reliability.

6. Conclusions and Outlook

Cemented carbide is extensively employed in extreme service environments, such as high-temperature cutting, mining and marine engineering, owing to its excellent hardness, superior wear resistance and outstanding thermal stability. In this work, the failure behaviors and mechanisms of cemented carbide in adhesive wear, abrasive wear, fatigue wear, oxidation wear, erosion wear, fretting wear and corrosion-wear coupled conditions are systematically summarized from the perspectives of material systems, microstructure characteristics and processing routes. The comprehensive analysis indicates that the tribological response and service degradation process of cemented

carbides are fundamentally governed by the synergistic interaction among the hard phase, the binder phase and the microstructure. Specifically, the type, size and spatial distribution of the hard phase determine the bearing capacity and wear resistance. The chemical composition and electrochemical activity of the binder phase dominate the interfacial stability. The microstructure scale, hard phase connectivity and microstructure uniformity jointly affect the crack initiation positions, crack propagation paths and the formation and evolution of the third-body layers, thereby regulating the macroscopic wear behavior. Consequently, the realization of multi-scale synergistic design and optimized matching among hard phases, binder phases and microstructures is essential for enhancing the comprehensive performance of cemented carbide.

Despite substantial progress in composition optimization, microstructural tailoring, and surface engineering in recent years, cemented carbides still face critical challenges under extreme service conditions. In high-temperature thermal-oxidation environments, such as high-speed cutting and aerospace hot-end components, the thermal softening of the binder phase and oxidation-induced interfacial embrittlement can significantly accelerate crack propagation and compromise long-term service stability. Under the corrosion and wear-corrosion coupling conditions of marine engineering and chemical equipment, localized dissolution and interfacial degradation of the binder phase will reduce the bearing capacity of the material skeleton, leading to a nonlinear increase in the wear rate. Under high-contact-stress environments involving impact loading and erosion/abrasive coupling, such as mining and slurry transport, microcrack accumulation, fatigue spalling, and third-body layer instability collectively dominate the failure behavior. More importantly, real service environments are typically accompanied by strong coupling among multiple physical fields, including thermal, mechanical, and chemical effects, resulting in pronounced time-dependent degradation and complex, path-dependent failure processes. Such coupled degradation behaviors remain difficult to be fully captured using conventional single-condition or short-duration laboratory tests.

Future research should be driven by the analysis of degradation mechanisms and the design of intelligent monitoring under multi-physical field coupling, with

representative extreme service conditions as the traction. At the material design level, it is necessary to further develop a high-entropy binder phase and a multiphase composite system, and to combine gradient microstructural architectures and micro-/nano-scale structural regulation to achieve synergistic improvements in strength, toughness, and corrosion resistance. At the surface engineering level, efforts should focus on surface modifications implemented on sintered cemented-carbide substrates, such as PVD/CVD-based protective films and functional surface texturing, to improve the service stability under extreme conditions. In addition, future studies need to establish a closed-loop control framework linking composition, structures, performances and conditions. On the one hand, standardized service simulation and long-term accelerated testing methodologies tailored for multi-physics coupling conditions should be developed to clarify key parameters and failure initiation criteria. On the other hand, combined with multi-scale numerical simulation and life prediction model, the quantitative description and pre-intervention of the degradation process are realized. With the continuous advancement of the above research directions, cemented carbides are expected to achieve higher service reliability and longer service life in extreme environments such as deep-sea energy, aerospace and high-end manufacturing.

Declaration of Competing Interest

The authors declare that they have no known competing financial interests or personal relationships that could have appeared to influence the work reported in this paper.

Data availability

Data will be made available on request.

References

[1] R.J.K. Wood, S. Herd, M.R. Thakare. A critical review of the tribocorrosion of cemented and thermal sprayed tungsten carbide [J]. *Tribol. Int.*, 2018, 119: 491-509.

[2] R. Yadav, A. Meena, S-Y. Lee, et al. Experimental tribological and mechanical

behavior of aluminium alloy 6061 composites incorporated ceramic particulates using Taguchi analysis [J]. *Tribol. Int.*, 2024, 192: 109243.

[3] K. Bobzin, C. Kalscheuer, M.P. Möbius, et al. Deformation behavior of high Al content CrAlON coatings with varying oxygen content[J]. *Surf. Coat. Tech.*, 2025, 496: 131639.

[4] J.B. Zhang, J.P. Wang, G.Q. Zhang, et al. A review of diamond synthesis, modification technology, and cutting tool application in ultra-precision machining [J]. *Mater. Des.*, 2024, 237: 112577.

[5] A. Bandyopadhyay, B. Heer. Additive manufacturing of multi-material structures [J]. *Mater. Sci. Eng. R. Rep.*, 2018, 129: 1-16.

[6] A.K. Bisht, R.O. Vaishya, R.S. Walia, et al. Nitrides ceramic coatings for tribological applications: A journey from binary to high-entropy compositions [J]. *Ceram. Int.*, 2024, 50: 8553-8585.

[7] C.Q. Fan, J.L. Sun, J. Zhao, et al. High entropy alloy bonded cemented carbides: Composition, processing, microstructure, properties and applications [J]. *Ceram. Int.*, 2024, 50: 37460-37503.

[8] C.S. Song, D.H. Xiang, B. Zhao, et al. Improving wear resistance and machining performance of diamond tools in ferrous metals cutting: A review [J]. *J. Mater. Process. Technol.*, 2024, 334: 118618.

[9] W.Q. Wang, W. Liu, Y. Zhang, et al. Precise measurement of geometric and physical quantities in cutting tools inspection and condition monitoring: A review [J]. *Chin. J. Aeronaut.*, 2024, 37(4): 23-53.

[10] H.R. Xing, P. Hu, C.J. He, et al. Design of high-performance molybdenum alloys via doping metal oxide and carbide strengthening: A review [J]. *J. Mater. Sci. Technol.*, 2023, 160: 161-180.

[11] Z.N. Cao, J.L. Sun, L.T. Meng, et al. Progress in densification and toughening of high entropy carbide ceramics [J]. *J. Mater. Sci. Technol.*, 2023, 161: 10-43.

[12] Y.T. Li, X.M. Chen, X.K. Zeng, et al. Hard yet tough and self-lubricating $(CuNiTiNbCr)C_x$ high-entropy nanocomposite films: Effects of carbon content on structure and properties [J]. *J. Mater. Sci. Technol.*, 2024, 173: 20-30.

[13]Z.X. Qiao, R. Yang, Y. Liu, et al. A feasible strategy to construct WC-Co-Cr/cu composite coating with good tribo-corrosion behavior and anti-fouling properties for marine applications [J]. *Wear.*, 2025, 564-565: 205738.

[14]A. Aramian, N. Razavib, Z. Sadeghiana, et al. A review of additive manufacturing of cermets [J]. *Addit. Manuf.*, 2020, 33: 101130.

[15]Z. Fathipour, M. Hadi, M.R. Maleki, et al. Effect of Binder on Oxidation Properties of Tungsten Carbides: A Review by a Conceptual Classification Approach [J]. *Ceramics.*, 2024, 7: 166-191.

[16]J.Y. Wei, L. Yang, G.J. Wang, et al. Research status of cutting machining NiTi shape memory alloys: a comprehensive review [J]. *Front. Mater.*, 2024, 11: 1431992.

[17]J. Kubarsepp, K. Juhani. Cermets with Fe-alloy binder: A review [J]. *Int. J. Refract. Met. H.*, 2020, 92: 105290.

[18]N.A. Shapagina, V.V. Dushik. Coatings Based on Refractory Materials for Corrosion and Wear Applications [J]. *Materials.*, 2024, 17: 5936.

[19]K.J. Li, X.F. Yang, S.K. Shen, et al. Research and prospect of novel WC-HEA cemented carbide [J]. *Int. J. Adv. Manuf. Technol.*, 2024, 130: 2085-2117.

[20]J. García, V. C. Ciprés, A. Blomqvist, et al. Cemented carbide microstructures: a review [J]. *Int. J. Refract. Met. H.*, 2019, 80: 40-68.

[21]L.P. Long, T. Chen, Q. Qin, et al. Microstructure and Properties of Gradient Ti(C, N)-Based Cermets by Powder Extrusion Additive Manufacturing [J]. *Metals.*, 2024, 14: 1161.

[22]Pooja, R. Pawar. A comprehensive investigation of Kingery type E3 (111) grain boundaries in TiC, TaC, and WC [J]. *Acta. Mater.*, 2024, 277: 120168.

[23]S. Kurbanbekov, Y. Kozhakhmetov, M. Skakov, et al. Properties, Advantages, and Prospects of Using Cobalt-Free Composites Based on Tungsten Carbide in Industry [J]. *Materials.*, 2025, 18: 129.

[24]E. Fransson, M. Gren, G. Wahnström. Complexions and grain growth retardation: First-principles modeling of phase boundaries in WC-Co cemented carbides at elevated temperatures [J]. *Acta. Mater.*, 2021, 216: 117128.

[25]T. Wu, C. Yang, L.T. Yu, et al. Microstructure characterization and high-temperature wear mechanism of high-entropy alloy matrix composite coating fabricated by laser cladding [J]. *Appl. Surf. Sci.*, 2024, 677: 161032.

[26]J. Pötschke, T. Säuberlich, A. Vornberger, et al. Solid state sintered nanoscaled hardmetals and their properties [J]. *Int. J. Refract. Met. H.*, 2018, 72: 45-50.

[27]P. Aghdasi, D.Y. Li. Electron work function guided tailoring of (W_{4-x}, M_x)C4/doped Ni matrix interfacial bonding: Insights from first-principles calculations [J]. *Acta. Mater.*, 2024, 283: 120511.

[28]Y.C. Wu, Z.Y. Lu, Y.Q. Qin, et al. Ultrafine/nano WC-Co cemented carbide: Overview of preparation and key technologies [J]. *J. Mater. Res. Technol.*, 2023, 27: 5822-5839.

[29]L. Yang, Y.J. Qian, S.Y. Lu, et al. In-situ synthesis of multi-element cemented carbides using the "trinity" method [J]. Mater. Lett., 2025, 389: 138340.

[30]P. Rose, J.K. Pallagani, S.B. Vummethala, et al. Environment-friendly process to net-shape tungsten carbide-cobalt components of precise and complex geometry [J]. *Int. J. Refract. Met. H.*, 2024, 124: 106826.

[31]C. Chen, B.Y. Huang, Z.M. Liu, et al. Additive manufacturing of WC-Co cemented carbides: Process, microstructure, and mechanical properties [J]. *Addit. Manuf.*, 2023, 63: 103410.

[32]F. Miranda, M.O.D. Santos, R. Condotta, et al. Additive Manufacturing of Tungsten Carbide (WC)-Based Cemented Carbides and Niobium Carbide (NbC)-Based Cermets with High Binder Content via Laser Powder Bed Fusion [J]. *Metals.*, 2024, 14: 1333.

[33]C.Y. Ma, T.N. Yang, Y.Q. Tang, et al. 3D Printing of cemented carbides: a review of techniques, defects, and post-processing [J]. *J. Mater. Res. Technol.*, 2025, 36: 9220-9245.

[34]X. Xia, C.Y. Ma, T.E. Yang, et al. Development of gradient cemented carbides with surface layers free of cubic phase via h-BN nitrogen source [J]. *Int. J. Refract. Met. H.*, 2025, 130: 107120.

[35]M. Slobodyan, E. Pesterev, A. Markov. A review of high-energy processing

techniques applied for additive manufacturing and surface engineering of cemented carbides and cermets [J]. *J. Manuf. Process.*, 2023, 105: 124-186.

[36] S.B. Zhao, L.J. Yang, Y.M. Huang, et al. A novel method to fabricate Ni/WC composite coatings by laser wire deposition: Processing characteristics, microstructural evolution and mechanical properties under different wire transfer modes [J]. *Addit. Manuf.*, 2021, 38: 101738.

[37] X.Y. Ren, H.B. Zou, Q.W. Diao, et al. Surface modification technologies for enhancing the tribological properties of cemented carbides: A review [J]. *Tribol. Int.*, 2023, 180: 108257.

[38] Z.C. Zhang, M.H. Sui, C.H. Li, et al. Residual stress of grinding cemented carbide using MoS_2 nano−lubricant [J]. *Int. J. Adv. Manuf. Technol.*, 2022, 119(9-10): 5671-5685.

[39] Q. Wan, X.Y. Tang, J.K. Yi, et al. Influence of laser machining process on the ablation amount and organizational properties of cemented carbide [J]. *Int. J. Refract. Met. H.*, 2025, 129: 107129.

[40] X. Tong, X.Y. Wang, P. Han, et al. Study on the surface performance strengthening of AlCrN coated cemented carbide by micro-texture laser preparation process [J]. *Opt. Laser. Technol.*, 2025, 181: 111819.

[41] L.R. Huang, J.L. Jiao, Y.H. Chen, et al. Influence of surface polishing technology on the surface properties and cutting performance of coated inserts for aluminum alloys [J]. *J. Manuf. Process.*, 2025, 149: 57-70.

[42] X.F. Yang, H.Y. Lin, Y.C. Chen, et al. Effect of AlTiN Coating Structure on the Cutting Performance of Cemented Carbide PCB Microdrills [J]. *Coatings.*, 2025, 15: 520.

[43] G.Y. Yan, Y.B. Sun, H. Wang, et al. Preparation and Mechanical Properties of Diamond Films on Textured WC-Co Substrate [J]. Adv. Eng. Mater., 2025, 27: 2402962.

[44] J. Chen, M.F. Gong, S.H. Wu. Cutting performance and wear mechanism of WC-Co ultrafine cemented carbide during cutting of HT250 gray cast iron [J]. *J. Ceram. Process. Res.*, 2015, 16(2): 244-248.

[45]L. Zhang, W.L. Song. Friction Behavior of Molybdenum Disulfide/Polytetrafluoroethylene-Coated Cemented Carbide Fabricated with a Spray Technique in Dry Friction Conditions [J]. *Coatings.*, 2025, 15: 324.

[46]H. Qiao, S.C. Zhu, S.X. Fan, et al. Tribological Performance of TiN-WS_2 Soft-Hard Multifunctional Composite Coatings Deposited by Magnetron Sputtering [J]. *Coatings.*, 2025, 15: 596.

[47]L.J. Sirtuli, F. Lindberg, D. Boing, et al. Impact of cutting tool and workpiece material on initial notch wear in turning [J]. *Wear.*, 2025, 570: 205942.

[48]Z.P. Hao, T.Y. Hou, J.G. Du, et al. Multi-scale predictive modeling of tool wear for machining Inconel 718 with cemented carbide tools [J]. *Tribol. Int.*, 2025, 208:110662.

[49]G.J. Liu, Z.C. Zhou, X. Qian, et al. Wear Mechanism of Cemented Carbide Tool in High Speed Milling of Stainless Steel [J]. *Chin. J. Mech. Eng.*, 2018, 31(1): 98.

[50]Y.Q. Su, T.B. Zhu, Y. Cheng, et al. Tribological properties and wear mechanisms of WC-ZrO_2-Al_2O_3-GNPs ceramics against typical counterparts [J]. *Wear.*, 2025, 564-565: 205705.

[51]M. Yahiaoui, J.-Y. Paris, J. Denape, et al. Wear mechanisms of WC-Co drill bit inserts against alumina counterface under dry friction: Part 2-Graded WC-Co inserts [J]. *Int. J. Refract. Met. H.*, 2015, 48: 65-73.

[52]J. Heinrichsa, M. Olssona, B. Almqvistc, et al. Initial surface failure and wear of cemented carbides in sliding contact with different rock types [J]. *Wear.*, 2018, 408-409: 43-55.

[53]R.K. Enneti, K.C. Prough. Wear properties of sintered WC-12%Co processed via Binder Jet 3D Printing (BJ3DP) [J]. *Int. J. Refract. Met. H.*, 2019, 78: 228-232.

[54]K. Bonnya, P.D. Baetsa, J. Vleugels, et al. Impact of Cr_3C_2/VC addition on the dry sliding friction and wear response of WC-Co cemented carbides [J]. *Wear.*, 2009, 267: 1642-1652.

[55]K. Zeng, X. Wu, F. Jiang, et al. A comprehensive review on the cutting and abrasive machining of cemented carbide materials [J]. *J. Manuf. Processes.*, 2023,

108: 335-358.

[56]V.K. Shankar, B.M. Kunar, C.S. Murthy, et al. Measurement of bit-rock interface temperature and wear rate of the tungsten carbide drill bit during rotary drilling [J]. *Friction.*, 2020, 8(6): 1073-1082.

[57]M. Antonov, R.Veinthal, D-L.Yung, et al. Mapping of impact-abrasive wear performance of WC-Co cemented carbides [J]. *Wear.*, 2015, 332-333: 971-978.

[58]X.Q. Zan, K.H. Shi, K.L. Dong, et al. Microstructure and Abrasive Wear Resistance of Mo2C Doped Binderless Cemented Carbide [J]. *Front. Mater.*, 2020, 7: 191.

[59]R.J. Cao, C.G. Lin, X.C. Xie, et al. Microstructure and mechanical properties of WC-Co-based cemented carbide with bimodal WC grain size distribution [J]. *Rare. Met.*, 2023, 42(8): 2809-2815.

[60]Y. Chen, L. Zhang, Z.Q. Zhong, et al. Effect of Substrates Characteristics on Tribological Behaviors of AlTiN-Based Coated WC-Co Cemented Carbides [J]. *Coatings.*, 2022, 12: 1517.

[61]S.Q. Fang, L. Llanes, D. Bähre. Wear Characterization of Cemented Carbides (WC-CoNi) Processed by Laser Surface Texturing under Abrasive Machining Conditions [J]. *Lubricants.*, 2017, 5(3): 20.

[62]C.Y. Feng, D. Chen, M.J. Xu, et al. Study of Solid Particle Erosion Wear Resistance of WC-Co Cemented Carbide [J]. *J. Fail. Anal. and Preven.*, 2020, 20(2): 543-554.

[63]N. Wu, F.D. Xue, J.Y. He, et al. Effect of tungsten carbide content on the tribological behavior of TiB2-TiC-based cermets [J]. *Wear.*, 2022, 498-499: 204333.

[64]K.L. Cai, J.L. Sun, H.B. Wang, et al. Synthesis, properties, and applications of functionally gradient cemented carbides [J]. *Prog. Solid. State. Chem.*, 2024, 74: 100454.

[65]X. Tong, S.C. Yang, X.L. Liu, et al. Friction, wear, and fatigue analysis for micro-textured cemented carbide [J]. *P. I. Mech. Eng. C-J. Mec.*, 2019, 233: 5989-6004.

[66]L. Zhang, W.L. Song, L. An, et al. Fabrication and Tribology Properties of Cr-

Coated Cemented Carbide under Dry Friction Conditions [J]. *Lubricants.*, 2023, 11: 278.

[67] W.L. Dong, X.F. Yang, F. Song, et al. Anti-friction and wear resistance analysis of cemented carbide coatings [J]. Int. J. Adv. Manuf. Tech., 2022, 122: 2795-2821.

[68] P.F. Cheng, N.N. Jiang, Z.Q. Wu. Effect of Nickel Element Diffusion on the Tribological Properties of Cemented Carbide Materials under High Temperature Condition [J]. *J. Mater. Eng. Perform.*, 2024, 34: 2788-2799.

[69] K.S. Li, G. Xu, X.B. Wen, et al. High-temperature friction behavior of amorphous carbon coating in glass molding process [J]. *Friction.*, 2021, 9(6): 1648-1659.

[70] Z.N. Zhang, Z. Li, SH. Pan, et al. Enhanced Strength and High-Temperature Wear Resistance of Ti6Al4V Alloy Fabricated by Laser Solid Forming [J]. *J. Manuf. Sci. E-T. Asme.*, 2022, 144: 111011.

[71] J.X. Deng. Friction and wear behaviour of $Al_2O_3/TiB_2/SiC_w$ ceramic composites at temperatures up to 800℃ [J]. *Ceram. Int.*, 2001, 27: 135-141.

[72] J.X. Deng, H. Zhang, Z. Wu, et al. Friction and wear behaviors of WC/Co cemented carbide tool materials with different WC grain sizes at temperatures up to 600 ℃ [J]. *Int. J. Refract. Met. H.*, 2012, 31: 196-204.

[73] S.A. Wohaibi, A.S. Mohammed, T. Laoui, et al. Tribological Characterization of Micron-/Nano-Sized WC-9%Co Cemented Carbides Prepared by Spark Plasma Sintering at Elevated Temperatures [J]. *Materials.*, 2019, 12: 920.

[74] Z.H. Wang, B. Yu, K. Liu, et al. Performance and wear mechanism of spark plasma sintered WC-Based ultrafine cemented carbides tools in dry turning of Ti-6Al-4V [J]. *Ceram. Int.*, 2020, 46: 20207-20214.

[75] P.X. Luo, Y.L. Liang, G.Y. He, et al. Effects of multi-layer graphene on the fracture toughness and wear resistance of WC-11Co cemented carbide [J]. J. Asian. Ceram. Soc., 2022, 10(2): 453-464.

[76] M.R. Derakhshandeh, M.J. Eshraghi, M. Razavi. Recent developments in the new generation of hard coatings applied on cemented carbide cutting tools [J]. *Int. J. Refract. Met. H.*, 2023, 111: 106077.

[77]S. Wang, H.Z. Liu B. Wu, et al. Exploring the ductile-regime machining on cemented carbide: A perspective review [J]. *J. Am. Ceram. Soc.*, 2025, 108(6): SI.

[78]Z. Zhao, X.N. Ni, Z.J. Hu, et al. A Short Review of Advancements in Additive Manufacturing of Cemented Carbides [J]. *Crystals.*, 2025, 15: 146.

[79]U. Beste, S. Jacobson. A new view of the deterioration and wear of WC/Co cemented carbide rock drill buttons [J]. *Wear.*, 2008, 264: 1129-1141.

[80]S.K. Sharma, B.V. Manoj Kumar, Y.W. Kim. Tribology of WC reinforced SiC ceramics: Influence of counterbody [J]. *Friction.*, 2019, 7(2): 129-142.

[81]K. Bose, R.J.K. Wood. High velocity solid particle erosion behaviour of CVD boron carbide on tungsten carbide [J]. *Wear.*, 2005, 258: 366-376.

[82]M. Antonov, J. Pirso, A. Vallikivi, et al. The effect of fine erodent retained on the surface during erosion of metals, ceramics, plastic, rubber and hard metal [J]. *Wear.*, 2016, 354-355: 53-68.

[83]P. Kulu, T. Pihl. Selection Criteria for Wear Resistant Powder Coatings Under Extreme Erosive Wear Conditions [J]. *J. Therm. Spray. Technol.*, 2002, 11(4): 517.

[84]V.P. Sharma, V. N. Shukla. Wear Behaviour of Cermet Coatings Deposited by Different Thermal Spray Techniques: A Review [J]. *Int. Res. J. Eng. Technol.*, 2016, 5: 637-639.

[85]A. Tewari. Load dependence of oxidative wear in metal/ceramic tribocouples in fretting environment [J]. *Wear.*, 2012, 289: 95-103.

[86]S.Q. Liu, J.Y. Fu, X. Shen, et al. Improved wear resistance of cemented carbide impact needle under high frequency micro-amplitude impact treated by high current pulsed electron beam [J]. *Wear.*, 2023, 518-519: 204632.

[87]S.Q. Liu, H.R. Xu, J.Y. Fu, et al. Impact fretting wear behavior of cemented carbide impact needle with surface modification [J]. *Mater. Des.*, 2025, 249: 113559.

[88]Q. Miao, W.J. Kuang, W.F. Ding, et al. Comparative Investigation on Fretting Wear of Nickel-Based Superalloy Surfaces Induced by Mechanical Polishing and Grinding [J]. *Tribol. Trans.*, 2023, 66(2): 279-291.

[89]A. Lenart, P. Pawlus, A. Dzierwa. The effect of steel disc surface texture in

contact with ceramic ball on friction and wear in dry fretting [J]. *Surf. Topogr-Metrol.*, 2018, 6(3): 034004.

[90] G. B. Raju, B. Basu. Influence of $MoSi_2$ Addition on Load-Dependent Fretting Wear Properties of TiB_2 Against Cemented Carbide [J]. *J. Am. Ceram. Soc.*, 2009, 92(9): 2059-2066.

[91] H. Qiu, X.Q. Li, C.L. Pan, et al. Effect of Mo_2C Addition on the Tribological Behavior of Ti(C, N)-Based Cermets [J]. *Materials*., 2023, 16: 5645.

[92] D.Q. Tan, X.Q. Yang, Q. He, et al. Failure Behavior of Cemented Carbide under Impact-Sliding Wear Conditions [J]. *Mater. Trans.*, 2021, 62(9): 1336-1342.

[93] Q. Zhan, F.Y. Luo, J. Huang, et al. Corrosion Resistance and Wear Behavior of Ni60/TiC and NbC Composite Coatings Prepared by Laser Cladding [J]. *Materials.*, 2025, 18: 2459.

[94] Y.S. Zhang, Z.G. Liu, C.G. Yang, et al. Microstructure and wear behavior of laser-cladded WC matrix composite coatings with different TiC/Ni contents on titanium alloys [J]. *Ceram. Int.*, 2025, 51: 27229-27242.

[95] G.L. Zhang, Y.C. Wang, Y. Liu, et al. Significant friction reduction of high-intensity pulsed ion beam irradiated WC-Ni against graphite under water lubrication [J]. *Friction.*, 2019, 7(3): 217-226.

[96] S. Wang, C. Ma, F. C. Walsh. Alternative tribological coatings to electrodeposited hard chromium: a critical review [J]. *Trans. Inst. Met. Finish.*, 2020, 98(4): 173-185.

[97] L.V. Duong, D.D. Phuong, N.B. Phuong, et al. Enhancing mechanical, tribological properties, and corrosion resistance of TiAlVN coatings through sputtering pressure variation [J]. *Ceram. Int.*, 2025, 51: 34089-34098.

[98] Y.H. Zhang, Y.N. Sun, J. Yang, et al. Tribological behavior of WC-NiMoCrFeCo coating in seawater environment: Long-term self-lubricating effects of a novel dynamic reaction product [J]. *Tribol. Int.*, 2026, 215: 111460.

[99] S. Friederichs, S. Lorenz. Characterization and comparison of cobaltbase and nickel-base alloys with iron-base intermetallic hard alloys used in wear protection [J]. *Pract. Metallogr.*, 2024, 61(3): 144-169.

[100] X.X. Liang, J.W. Yan, C.M. Li, et al. Water lubrication friction and wear behaviors of WC hard alloy and metal pairs [J]. *Wear.*, 2025, 571: 205795.

[101] S.L. Nie, W.H. Xu, F.L.Yin, et al. Investigation of the tribological behaviour of cermets sliding against Si_3N_4 for seawater hydraulic components applications [J]. *Surf. Topogr-Metrol.*, 2019, 7(4): 045025.

[102] D.S. Guedes, T.P.D. Freitas. On The Mechanical and Electrochemical Performance of High Corrosion Resistance WC-Ni-Based Composites [M]. 2022.

[103] X.X. Liang, S.H. Qi, Z.Y. Yang, et al. Friction and wear behavior of cemented carbide self-matching pairs under different water lubrication conditions [J]. *Wear.*, 2023, 523: 204832.

[104] X. Zhai, H. Ji, S.L. Nie, et al. Effect of different Ni concentration on the corrosion and friction properties of WC-hNi/SiC pair lubricated with seawater [J]. *Int. J. Refract. Met. H.*, 2022, 102: 105727.

[105] E. Bosi, A. Meghwal, M. Hourmand, et al. First report of agglomerated and sintered carbide-high-entropy alloy composite thermal spray coating [J]. *Scr. Mater.*, 2025, 260: 116591.

[106] G. Wang, C. Xing, F. Tao, et al. Enhancement in the corrosion resistance of WC coatings by adding a Fe-based alloy in simulated seawater [J]. *Surf. Coat. Tech.*, 2016, 305: 62-66.

[107] Q.Z. Xu, L.Y. Chen, M.J. Sun, et al. A comparative study of corrosion property, tribological behavior and cutting performance of tool materials for the cutting of marine high-strength steels in the marine environment [J]. *P. I. Mech. Eng. B-J. Eng.*, 2021, 235(1-2): 98-111.

[108] C.T. Wang, Y.W. Ye, X.Y. Guan, et al. An analysis of tribological performance on Cr/GLC film coupling with Si_3N_4, SiC, WC, Al_2O_3 and ZrO_2 in seawater [J]. *Tribol. Int.*, 2016, 96: 77-86.

[109] Y. H. Zhang, Y. N. Sun, X.J. Fan, et al. Corrosion behavior of WC-NiMoCrFeCo coating in seawater environment: Positive corrosion inhibition of a novel dynamic reaction product [J]. *Chem. Eng. J.*, 2025, 507: 160568.

[110] W.M. Zhou, P.F. Feng, W. Ji, et al. Multiscale analysis on the wear process

of cemented carbide tools during titanium alloy machining [J]. *Friction.*, 2005, 13(3): 9440921.

[111] X.W. Zhang, Q.Z. Mao, Z.F. Yu, et al. Multi-layer structure improves wear and corrosion resistance of chromium [J]. *Surf. Coat. Tech.*, 2025, 508: 132165.

[112] L. Shan, Y.X. Wang, J.L. Li, et al. Tribological behaviours of PVD TiN and TiCN coatings in artificial seawater [J]. *Surf. Coat. Tech.*, 2013, 226: 40-50.

[113] Z.X. Guo, J. Xiong, W.C. Wan, et al., Effect of Binder Content on the Erosive Wear of Ti(C, N)-Based Cermet in SiO_2 Particle-Containing Simulated Seawater [J]. *Int. J. Appl. Ceram. Technol.*, 2014, 11(6): 1045-1053.

[114] L. Zhang, Z.F. Huang, W.Q. Jie, et al. Effect of impact angle on wear behavior of Mo_2NiB_2-Ni cermets with different Ni content [J]. *Ceram. Int.*, 2022, 48: 16944-16955.

[115] A. Tiwari, S. Seman, G. Singh, et al. Nanocrystalline Cermet Coatings for Erosion-Corrosion Protection [J]. *Coatings.*, 2019, 9: 400.

[116] K. Bobzin, M. O¨ te, T.F. Linke, et al. Wear and Corrosion Resistance of Fe-Based Coatings Reinforced by TiC Particles for Application in Hydraulic Systems [J]. *J. Therm. Spray.Technol.*, 2016, 25(1-2): 365-374.

[117] D.L. Yung, M. Antonov, R. Veinthal, et al. Wear behaviour of doped WC-NI based hard metals tested by four methods [J]. *Wear.*, 2016, 352-353: 171-179.

[118] L. Zhang, W. Tian, Y. Chen, et al. Fine platelet-like grained WC-Co cemented carbides: Preparation, characterization, properties and application in PVD coating substrates [J]. *Int. J. Refract. Met. H.*, 2017, 64: 135-142.

[119] M.Y. Ma, Y.C. Diao, K. Wang, et al. Nanocrystalline microstructure enhanced mechanical properties and cutting performance of WC-10Co-Ti(C, N) gradient cemented carbides [J]. *Mater. Charact.*, 2024, 209: 113708.

[120] M. Walbrühl, D. Linder, J. Ågren, et al. Alternative Ni-based cemented carbide binder-Hardness characterization by nano-indentation and focused ion beam [J]. *Int. J. Refract. Met. H.*, 2018, 73: 204-209.

[121] J. Lu, S.W. Tang, H. Zhang, et al. Preparation and mechanical properties of SiC_w-reinforced WC-10Ni_3Al cemented carbide by microwave sintering [J].

Ceram. Int., 2023, 49: 21587-21601.

[122] Y.C. Diao, M.Y. Ma, G.J. Li, et al. $L1_2$ strengthening of WC-CoNiFe cemented carbides by spark plasma sintering [J]. *Ceram. Int.*, 2024, 50: 56135-56143.

[123] J.Y. Liu, K.Y. Hao, R.N. Zhou, et al. Enhancing the corrosion resistance of cemented carbides using CoCrNi binders in simulated drilling fluids [J]. *Ceram. Int.*, 2025, 51: 11690-11701.

[124] J.J. Roaa, E. Jimenez-Pique, C. Vergea, et al. Intrinsic hardness of constitutive phases in WC-Co composites: Nanoindentation testing, statistical analysis, WC crystal orientation effects and flow stress for the constrained metallic binder [J]. *J. Eur. Ceram. Soc.*, 2015, 35(13): 3419-3425.

[125] M. Christensen, G. Wahnström. Strength and reinforcement of interfaces in cemented carbides [J]. *Int. J. Refract. Met. H.*, 2006, 24(1-2): 80-88.

[126] Y. Liu, X.F. Li, J.H. Zhou, et al. Effects of Y_2O_3 addition on microstructures and mechanical properties of WC-Co functionally graded cemented carbides [J]. *Int. J. Refract. Met. H.*, 2015, 50: 53-58.

[127] M. Li, M.F. Gong, Z.L. Cheng, et al. Novel WC-Co-Ti_3SiC_2 cemented carbide with ultrafine WC grains and improved mechanical properties [J]. *Ceram. Int.*, 2022, 48: 22335-22342.

[128] X.F. Li, Y. Liu, W. Wei, et al. Influence of NbC and VC on microstructures and mechanical properties of WC-Co functionally graded cemented carbides [J]. *Mater. Des.*, 2016, 90: 562-567.

[129] H.L. Tian, C.L. Wang, M.Q. Guo, et al. Microstructures and high-temperature self-lubricating wear-resistance mechanisms of graphene-modified WC-12Co coatings [J]. *Friction.*, 2021, 9(2): 315-331.

[130] M. Ostolaza, A. Zabala, J.I. Arrizubieta, et al. High-temperature tribological performance of functionally graded Stellite 6/WC metal matrix composite coatings manufactured by laser-directed energy deposition [J]. *Friction.*, 2024, 12(3): 522-538.

[131] S. Dosta, M. Couto, J.M. Guilemany. Cold spray deposition of a WC-25Co

cermet onto Al7075-T6 and carbon steel substrates [J]. *Acta. Mater.*, 2013, 61(2): 643-652.

[132] G.P. Lin, Z.B. Cai, B.W. Lu, et al. Enhanced wear resistance of laser cladded WC-Ni composite coatings by picosecond laser surface texturing [J]. *Tribol. Int.*, 2025, 110517.

[133] L. Liang, J.D. Yuan, X.Q. Li, et al. Wear behavior of the micro-grooved texture on WC-Ni_3Al cermet prepared by laser surface texturing [J]. *Int. J. Refract. Met. H.*, 2018, 72: 211-222.

[134] K.D. Zhang, J.X. Deng, R. Meng, et al. Influence of laser substrate pretreatment on anti-adhesive wear properties of WC/Co-based TiAlN coatings against AISI 316 stainless steel [J]. *Int. J. Refract. Met. H.*, 2016, 57: 101-114.

[135] Y.L. Liu, J. Cheng, B. Yin, et al. Study of the tribological behaviors and wear mechanisms of WC-Co and WC-Fe_3Al hard materials under dry sliding condition [J]. *Tribol. Int.*, 2017, 109: 19-25.

[136] V. Rajinikanth, K. Venkateswarlu. An investigation of sliding wear behaviour of WC-Co coating [J]. *Tribol. Int.*, 2011, 44(12): 1711-1719.

Kaipeng Zhang. He received his B.S. degree in Industrial Engineering in 2019 and his Ph.D. degree in Mechanical Engineering in 2025, both from Wuhan University of Technology. He is currently a postdoctoral researcher at the State Key Laboratory of Tribology in Advanced Equipment at Tsinghua University. His research interests include bio-inspired surface texturing, fluid-solid coupled lubrication, and the tribological behavior of advanced materials. He has published more than 30 SCI papers in Tribology International, Friction, and Wear.

Pengpeng BAI. He received his Ph.D. in Materials Science and

Engineering from China University of Petroleum (Beijing) in 2017. He is currently an Assistant Research Fellow in the Department of Mechanical Engineering, Tsinghua University. His research has long been focused on applied fundamental studies of wide-temperature-range lubricating materials, interfacial tribology, and corrosion.

Hui Cao. Dr. Hui Cao is an Assistant Research Fellow in State Key Laboratory of Tribology in Advanced Equipment, Tsinghua University. He has long been engaged in both fundamental and applied research on friction, wear, and lubrication. His research interests cover mixed lubrication theory and mechanisms, adhesive wear mechanisms, running-in process mechanisms and optimization, tribo-dynamics of key mechanical components such as bearings and precision reducers. He has published more than 20 SCI papers in Tribology International, Friction, and Journal of Tribology etc.

Yonggang Meng. He received his M.S. and Ph.D. degrees in mechanical engineering from Kumamoto University, Japan, in 1986 and 1989, respectively. He joined the State Key Laboratory of Tribology at Tsinghua University in 1990. His current position is a professor, and his research areas cover the tribology of MEMS and hard disk drives, active control of friction and interfacial phenomena, and nano manufacturing